Polarforschung 63 (2/3): 63–99, 1993 (erschienen 1995)

Structural Investigations in Proterozoic to Lower Palaeozoic Rocks in the Read Mountains and Haskard Highlands of the Shackleton Range, Antarctica

By Hans-Martin Braun*

Abstract: Studies on macroscopic rock deformation and microfabrics of the basement rocks of the Shackleton Range, Antarctica, confirm two major tectonometamorphic events. During the mid-Proterozoic, the basement was affected by prograde metamorphism reaching at least amphibolite facies conditions, and syn-metamorphic ductile deformation. In several outcrops in the Read Mountains (southern Shackleton Range), relations between deformation, metamorphism, and intrusive activity are reconstructed in detail. Proterozoic tectonometamorphism terminated with uplift and erosion of the basement, followed by deposition of the Eocambrian Watts Needle Formation, a thin sequence of epicratonic sediments. Information about the early history of basement rocks in the Haskard Highlands (northern Shackleton Range) is not as detailed, but a major tectonometamorphic event during the mid-Proterozoic can be demonstrated as well.

During the Cambrian and Early Ordovician, basement and cover sediments in the Read Mountains were overthrust by the so-called Mount Wegener Nappe (Mt. Wegener Formation). Structures in the underlying rocks indicate S or SE transport of the nappe. Final uplift, and partial erosion of the nappe unit in the central Read Mountains („Mount Wegener Window") are probably related to large-scale upright folding. At the same time, sedimentary rocks in the northern Haskard Highlands suffered amphibolite-facies metamorphism and intense rotational deformation, leading to a stack of several structural units. By defining major zones of NW directed tectonic transport (thrust planes) and characteristic microstructures, the lithostratigraphic setting originally inferred for this region is slightly modified.

The structural history of the Shackleton Range, as derived from this study, is compared with that of northern Victoria Land, the central Transantarctic Mountains, and Neuschwabenland (western Dronning Maud Land). After discussing the early Palaeozoic tectonics of the Shackleton Range within the classical concept of the Ross orogen, alternative geotectonic interpretations are suggested that are based on the hypothetical,"SWEAT" reconstruction of continents.

Zusammenfassung: Untersuchungen makroskopischer und mikroskopischer Gefüge im Grundgebirge der Shackleton Range belegen zwei Hauptphasen tektonometamorpher Aktivität. Parallel zu mindestens amphibolit-fazieller Metamorphose unterlagen die Gesteine im Mittleren Proterozoikum intensiver duktiler Deformation. Für Aufschlüsse in den Read Mountains (südliche Shackleton Range) können detaillierte Angaben über die wechselseitigen Beziehungen zwischen Deformation, Metamorphose, und der Platznahme von Intrusionen gemacht werden. Die proterozoische Tektonometamorphose endet hier mit dem Aufstieg und der Erosion des Grundgebirges, und der Ablagerung der eokambrischen Watts Needle Formation, einer geringmächtigen Abfolge epikratonischer Sedimente. In der nördlichen Shackleton Range (Haskard Highlands) sind die Kenntnisse über frühe Ereignisse im Grundgebirge nicht so detailliert wie im Süden, doch kann eine proterozoische Überprägung der Gesteine auch hier belegt werden.

Während des Kambriums und des frühen Ordoviziums wurden Grundgebirge und Decksedimente der Read Mountains von der sogenannten Mount-Wegener-Decke (Mount Wegener Formation) überfahren. Gefüge in den autochthonen Gesteinen deuten auf einen von N (-NW) nach S (-SE) gerichteten Transport der Decke hin. Abschließende Heraushebung und teilweise Erosion der Decke in den zentralen Read Mountains („Read-Fenster") sind vermutlich an eine großräumige, aufrechte Faltung gebunden. Während desselben Zeitraums wurden Sedimente in den nördlichen Haskard Highlands unter amphibolitfaziellen Bedingungen deformiert und zu einem Stapel mehrerer Struktureinheiten übereinandergeschoben. Mit Hilfe der Lokalisierung größerer Bewegungshorizonte, auf denen NW-gerichtete Überschiebungen stattfanden, und der Untersuchung charakteristischer Mikrogefüge, kann die ursprünglich für diese Region vorgeschlagene lithostratigraphische Gliederung leicht modifiziert werden.

Abschließend wird die strukturelle Entwicklung der Shackleton Range, wie sie hier erarbeitet wurde, mit Erkenntnissen aus Nord-Viktorialand, dem zentralen Transantarktischen Gebirge, und Neuschwabenland (westliches Königin-Maud-Land) verglichen. Nach einer Diskussion der früh-paläozoischen Deckentektonik im Rahmen des Ross-Orogens im klassischen Sinne werden alternative Interpretationen aufgezeigt, die sich aus plattentektonischen Rekonstruktionen gemäß der neuen „SWEAT"-Hypothese ergeben.

1. INTRODUCTION

The Shackleton Range is situated at about 80 °S close to the SE boundary of the Filchner Ice Shelf (Fig. 1). Results of the first geological studies in the area, including some general descriptions of tectonic structures, have been published by CLARKSON (1982a, b, 1983), HOFMANN & PAECH (1983), PAECH (1985), and MARSH (1983a, b, 1984). The general pattern of geological units in the Shackleton Range, as derived from these papers, is shown in Fig. 1. Due to the reconnaissance level of exploration, however, interpretations dealing with the tectonometamorphic evolution of the Shackleton Range have remained rather speculative.

During the „Geological Expedition into the Shackleton Range" (GEISHA) in 1987/88, the author had the opportunity to visit several areas in the Read Mountains (see Fig. 2) to study the medium- to high-grade metamorphic rocks of the Read Group, and sediments of the Watts Needle Formation. In addition, metamorphic basement and supracrustal rocks in the northern Haskard Highlands (Fig. 1) were investigated. The aim of the present paper is to identify and describe structures and fabrics that are characteristic of certain units and tectonometamorphic events. The relative and absolute timing of these events in relation to the overall geological history of the Shackleton Range will also be analyzed.

* Hans-Martin Braun, Geologisch-Paläontologisches Institut, Johann Wolfgang Goethe-Universität, Senckenberganlage 32-34, D-60325 Frankfurt am Main, Germany.
Manuscript received 14 April 1994; accepted 30 September 1994

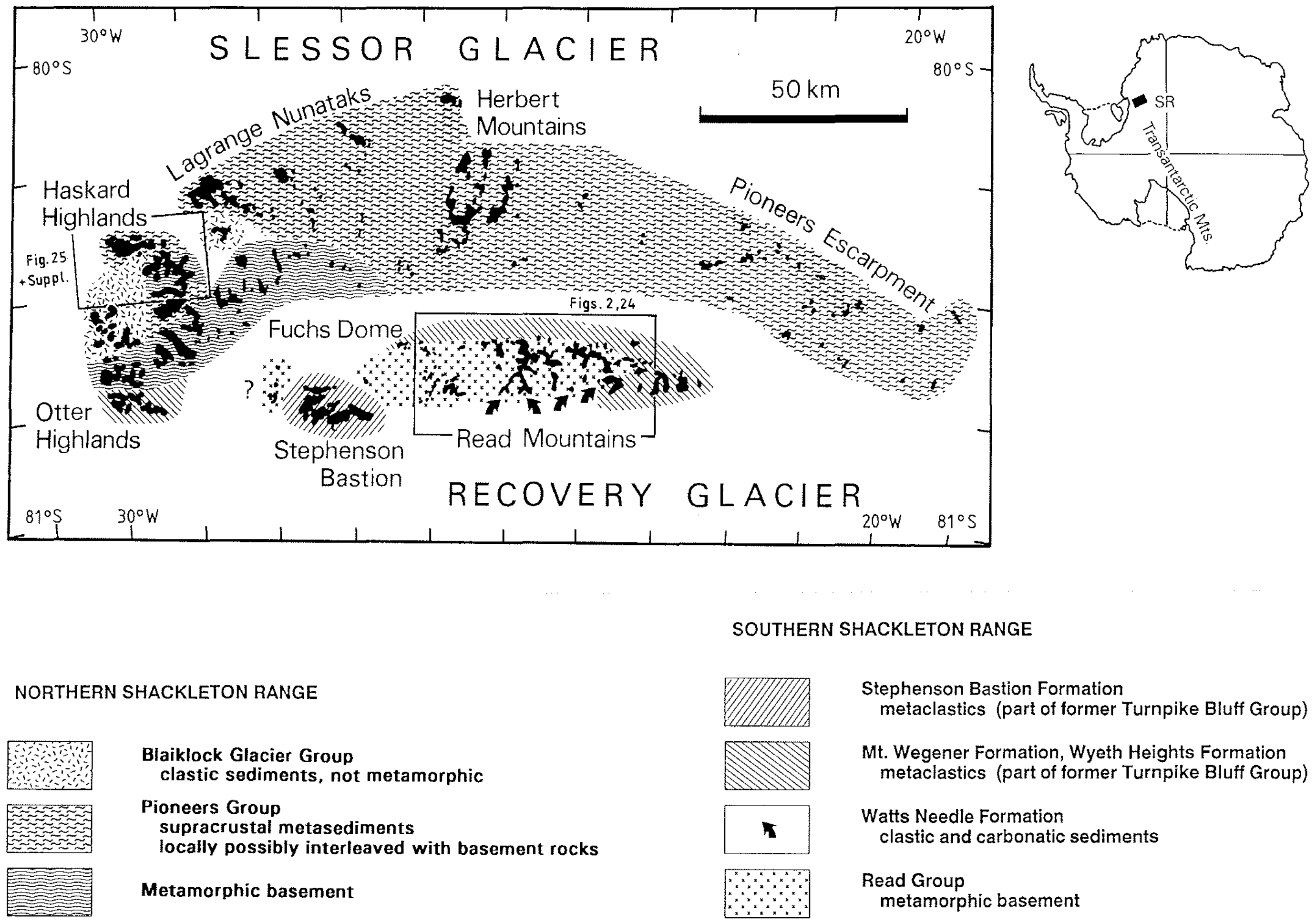

Fig. 1: The Shackleton Range, Antarctica, showing the main topographical features and geological units.

Abb. 1: Übersicht über Topographie und Geologie der Shackleton Range, Antarktis.

2. TECTONOMETAMORPHIC EVOLUTION OF THE READ MOUNTAINS

2.1 *General outline*

Data and maps from previous studies provide a rough impression of the overall structure of the Read Mountains (e.g. Clarkson 1982a). Crystalline rocks of the Read Group form a lenticular body surrounded by clastic sediments and measuring about 70 km from E to W. The foliation in the basement rocks dips N in the northern part, and S in the southern part. Hofmann & Paech (1983) and Paech (1985), therefore, assumed a large E-W-striking anticline in the Read Mountains. In the central and southern Read Mountains, the contact between the crystalline basement and the sedimentary cover is exposed at only a few locations (Watts Needle area, Nicol Crags, Mount Wegener; Fig. 2). Sediments of the Watts Needle Formation are found between the Read Group basement and the metaclastic rocks of the Mount Wegener Formation. Marsh (1983b), on the basis of the sequence of lithological units at Watts Needle,was the first to mention the possibility of thrusting in the Read Mountains. Indeed, investigations during the GEISHA expedition led to the identification of the so-called „Mount Wegener Nappe“ (Buggisch et al. 1994a) . According to this model, the Mount Wegener Formation represents an allochthonous unit that overrode both the metamorphic basement and the Watts Needle Formation sediments, truncating the latter at different levels (Braun et al. 1988, Roland et al. 1988, Buggisch et al. 1990, Kleinschmidt & Braun 1991, Buggisch et al. 1994a, b). The large block of crystalline rock at the top of Watts Needle and some smaller lenses at Mount Wegener are thought to have been tectonically transported within the base of the nappe. The central Read Mountains today form a classical window structure („Read Window“, Buggisch et al. 1994a).

The present study deals with following aspects of the geology of the Read Mountains:
- The structural evolution of the Read Mountains, as derived from detailed investigations within the crystalline basement and the Watts Needle Formation.
- The thrust-induced deformation structures in the units below the Read Nappe.
- The kinematics of nappe transport, as deduced from the corresponding fabrics of the underlying units.
- The correlation between deformation structures and metamorphic events.

Due to limited time in the field, work in the Read Mountains

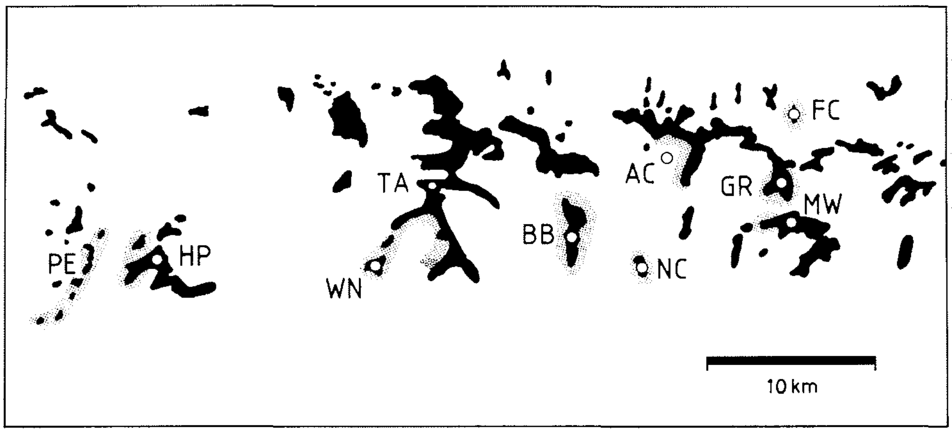

Fig. 2: Areas in the Read Mountains in the southern Shackleton Range mentioned in this study: PE = Poldervaart Edge, HP = Hatch Plain, WN = Watts Needle, BB = Beche Blade, AC = Arkell Cirque, NC = Nicol Crags, MW = Mount Wegener, GR = Gora Rudachenka, FC = Flett Crags, TA = The Ark (for location of Read Mountains, see Fig. 1).

Abb. 2: Im Rahmen der vorliegenden Arbeit behandelte Gebiete der südlichen Shackleton Range (vergl. Abb. 1): PE = Poldervaart Edge, HP = Hatch Plain, WN = Watts Needle, BB = Beche Blade, AC = Arkell Cirque, NC = Nicol Crags, MW = Mount Wegener, GR = Gora Rudachenka, FC = Flett Crags, TA = The Ark.

was concentrated on several distinct outcrop areas in which representative information on the aspects mentioned above could be expected (Fig. 2).

2.2 *Description of tectonic structures*

2.2.1 The Watts Needle region

2.2.1.1 Read Group

Foliation planes of the Read Group are parallel to the large-scale layering of the rocks. They dip subvertically NW on the western slope of Watts Needle and have a moderate westerly dip on its eastern slope. About 4 km E of Watts Needle, the foliation dips E at moderate angles. Pegmatitic layers, reaching several metres thickness on the E side of Watts Needle, show biotites oriented parallel to the foliation of the surrounding metamorphics. The same is true for fine- to medium-grained granitic gneisses close to The Ark, north of Watts Needle.

East of the Watts Needle summit, rheologically competent layers have been uniaxially stretched, forming typical pinch-and-swell structures (Ramberg 1955). Individual boudins measure 0.5-1 m in the X-direction of deformation (Fig. 3). The „pinch" zones - assumed to indicate the Y-direction - dip about 30 °W. The complete lack of boudin rotation indicates extension parallel to the layering and a coaxial deformational regime.

During an early stage of deformation, quartz veins and pegmatites were isoclinally folded with axial planes marked by large biotite flakes parallel to the foliation (Fig. 4). NE of Watts Needle, a fine net of feldspathic veins (agmatitic neosome, see below) shows ptygmatic folding. Fold axes generally plunge SW or NE at gentle angles at Watts Needle, and somewhat steeper NE to E several kilometres further east (Fig. 5).

A second, younger fold generation on the eastern slope of Watts Needle shows sharp, almost kink-like hinges. S- or Z-shaped double folds commonly occur, with short limbs several dm long. On the basis of the sense of these double folds, an eastern vergency prevails. The fold axes dip mostly N to NNE. Widely spaced, second-generation foliation planes are parallel to the subvertical axial planes.

Fig. 3: Non-rotational boudinage (pinch-and-swell structure) of a competent quartzo-feldspathic layer within Read Group metamorphics; Watts Needle, Read Mountains, southern Shackleton Range (view to the W); length of hammer is 60 cm.

Abb. 3: Irrotationale Boudinage einer kompetenten, quarz-feldspat-reichen Lage innerhalb der Read Group („pinch and swell"-Struktur). Watts Needle, Read Mountains, südliche Shackleton Range; Blick nach Westen, Länge des Hammers = 60 cm.

Two sets of lineations have been observed. An older mineral lineation is developed only W of the Watts Needle summit. If the lineations are rotated on the stereogram to compensate for late tilting, then the lineation and the X-axis of boudinage are found to have the same direction. Small-scale crenulations in rocks rich in phyllosilicates or actinolite represent the second generation of linear fabrics. After rotation, this crenulation lineation parallels the axes of isoclinal folding.

West of the Watts Needle summit, ENE-WSW and NNE-SSW-striking planes define an almost orthogonal joint system (Fig. 6). For a vertical, WNW-ESE-striking fault zone on the E side of Watts Needle, deflected foliation planes indicate relative downthrow of the NW block. On the opposite side of Watts Needle, a steep, N-dipping fault plane is filled with fine-grained fault gouge.

2.2.1.2 Watts Needle Formation

The sandstone member of the Watts Needle Formation rests unconformably on top of the Read Group basement. Subhori-

Fig. 4: Folded pegmatite vein within Read Group metamorphics. Note internal axial plane foliation (marked by large biotites), which is roughly parallel to the foliation of the country rock. Narrow granitic vein was emplaced after the folding event. Watts Needle, Read Mountains, southern Shackleton Range; length of pen is about 15 cm.

Abb. 4: Verfalteter Pegmatitgang innerhalb der Read Group. Große, achsenebenen-parallel gewachsene Biotite und die Schieferung der umgebenden Metamorphite sind ungefähr gleich orientiert. Nach der Verfaltung drang ein schmaler granitischer Gang ein. Watts Needle, Read Mountains, südliche Shackleton Range; Länge des Stiftes = 15 cm.

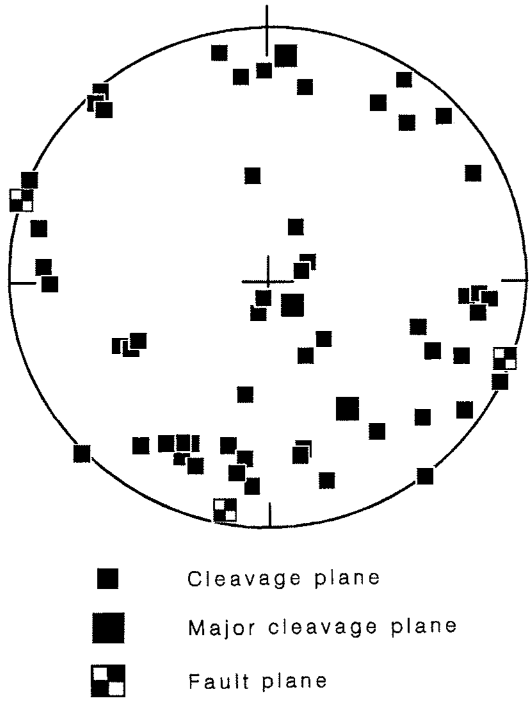

Fig. 6: Schmidt net projection of brittle deformation structures in Read Group metamorphics. Watts Needle and ridge further E, Read Mountains, southern Shackleton Range.

Abb. 6: Darstellung bruchhafter Deformationsgefüge innerhalb der Read Group im Schmidt'schen Netz; Watts Needle und ein weiter östlich gelegener Rücken, Read Mountains, südliche Shackleton Range.

zontal bedding and sedimentary structures (e.g. crossbedding) are preserved without any macroscopic sign of ductile deformation, which is also true for the overlying stromatolitic carbonate layers. A large number of small, almost vertical cleavage planes cut these basal sediments. The dominance of NE-SW-striking cleavage planes may be genetically related to SE-directed thrusting on top of the Watts Needle Formation (see 2.4).

The present boundary between the sandstone and stromatolite members of the Watts Needle Formation and the overlying carbonatic schists represents the original, sedimentary contact. The schists are intensely folded with wavelengths of 5-20 m, and many subordinate folds on the order of several m to several dm. They have NE-plunging axes and subhorizontal axial planes (Fig. 7). Long to short limb relations indicate tectonic transport to the SE. Veins oblique to the XY-plane of overall deformation possibly represent tension gashes. Ductile shears inclined to the NNE or SSW contain fine-grained mylonitic gouge.

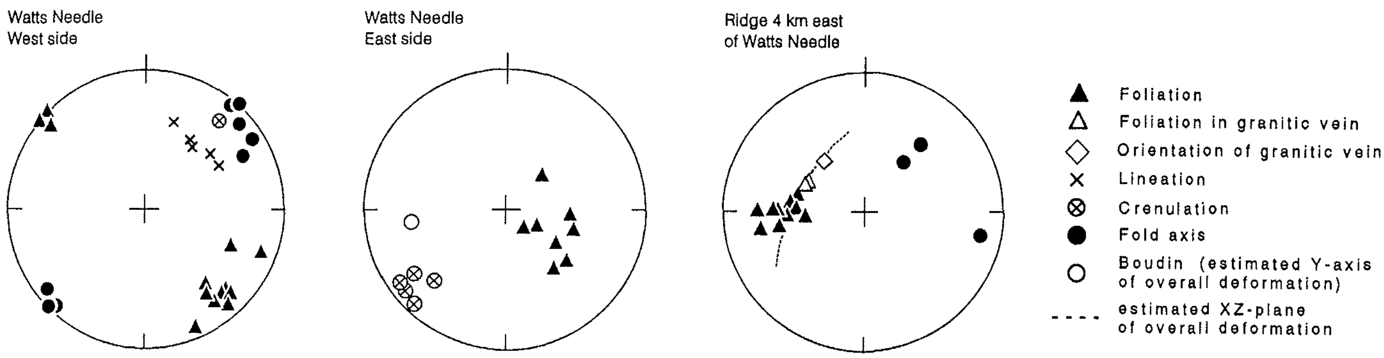

Fig. 5: Schmidt net projection of ductile deformation structures in Read Group metamorphics; Watts Needle and ridge further E, Read Mountains, southern Shackleton Range.

Abb. 5: Darstellung duktiler Deformationsgefüge innerhalb der Read Group im Schmidt'schen Netz; Watts Needle und ein weiter östlich gelegener Rücken, Read Mountains, südliche Shackleton Range.

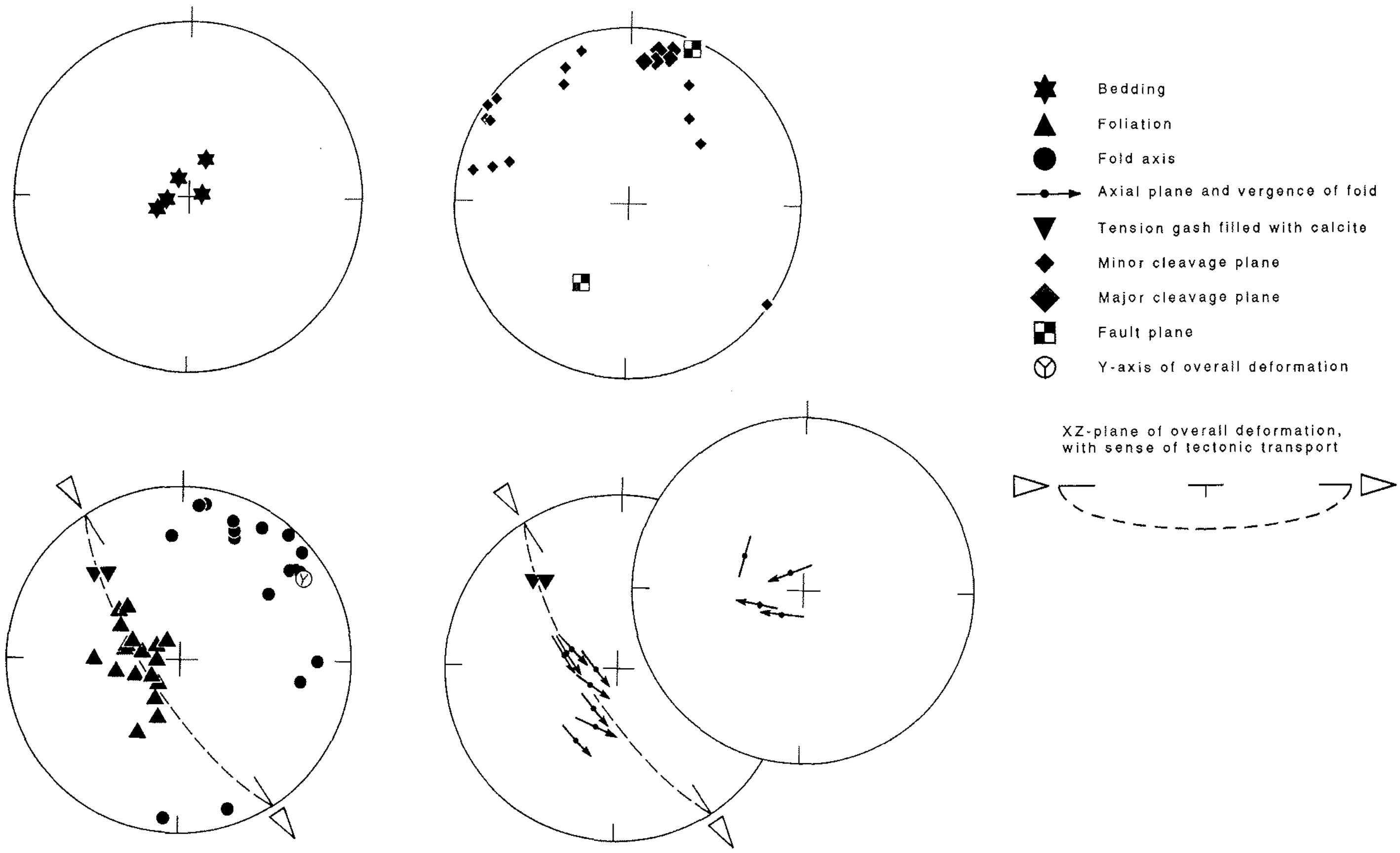

Fig. 7: Schmidt net projection of sedimentary layers and deformation structures within the Watts Needle Formation, Watts Needle area, Read Mountains, southern Shackleton Range.

Abb. 7: Schichtflächen und Deformationsgefüge innerhalb der Watts Needle Formation im Schmidt'schen Netz; Watts Needle, Read Mountains, südliche Shackleton Range.

2.2.1.3 Crystalline rocks on top of the Watts Needle Formation

In contrast to the metamorphics below the Watts Needle Formation, continuous foliation planes are rare in the block of crystalline rock on top of the metasediments. They dip to the north in the immediate summit area and curve into the subhorizontal sole plane (Fig. 8). The whole lower part of the unit is disrupted by irregularly oriented fractures on all scales. The brecciated crystalline rocks consist chiefly of quartz, biotite, chlorite, and some relics of large feldspars. The original rock was probably a porphyritic granite.

2.2.2 Beche Blade

A porphyritic granite containing feldspars several cm long crops out on the N and NE sides of Beche Blade. To the NW, it is in contact with granodiorites that - as far as can be seen from the ground - also form the roof of the granite body. Layered metamorphics are exposed on the E side. Hornfels xenoliths in the granite indicate that it intruded both the granodiorites and the surrounding metamorphics. The southern part of Beche Blade consists of quartzofeldspathic metamorphic rocks that are cut by white or pink aplites, especially in the SE part.

Since the feldspars in the porphyritic granites are randomly oriented, a post-deformational age of intrusion is suggested. In contrast, biotite and hornblende in the granodioritic rocks are parallel to the steeply N- or S-dipping foliation of the surrounding metamorphics. The gneissic granites in the central Beche Blade show nebulous foliation streaks. Layering and foliation form tight folds with SW-plunging axes and northern vergency (Fig. 9). Layering and foliation in the metamorphic rocks of the southern Beche Blade dip southward at medium angles. Oriented growth of actinolite creates a NNE-SSW lineation . Shear zones use aplitic veins as slip planes.

Most of the brittle fabrics encountered strike E-W and are subvertical. On the E side of Beche Blade, a fault zone 0.5 m thick shows fractures filled with epidote. In the western part, intense retrograde alteration is due to hydrothermal fluid circulation along cleavage and fault planes.

2.2.3 Arkell Cirque

Cliffs marking the E side of Arkell Cirque (Fig. 10"A") show two different lithologies. The southernmost part of the outcrop consists of gray, fine-grained granite in contact with biotitic gneisses south of the first col. A large number of pegmatitic veins dissect both the granite and the surrounding metamorphics. Post-intrusive folding has S-plunging axes, while weak crenu-

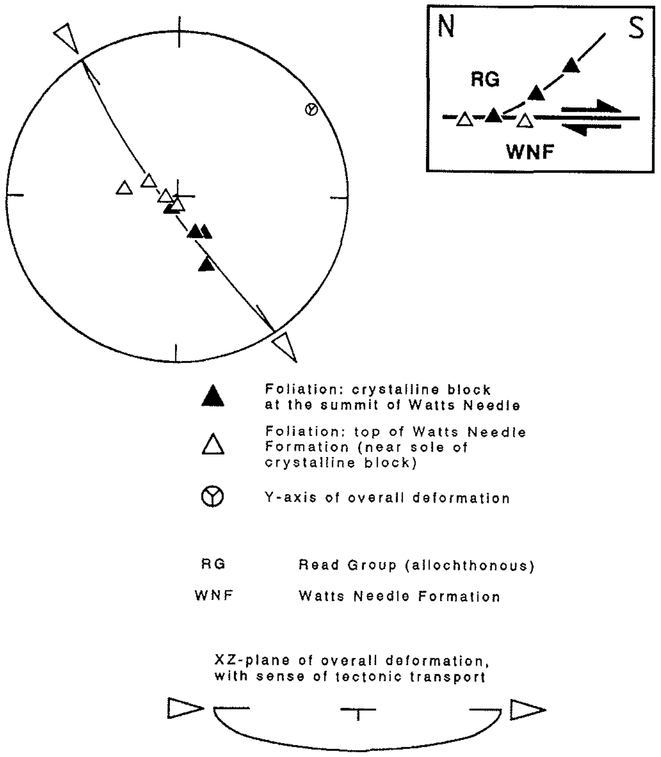

Fig. 8: Schmidt net projection of foliation planes in the crystalline block on the Watts Needle summit and in its sole thrust plane; Read Mountains, southern Shackleton Range.

Abb. 8: Schieferungsflächen an der Basis, und innerhalb des Kristallin-Blocks, der den Gipfel der Watts Needle aufbaut. Darstellung im Schmidt'schen Netz; Read Mountains, südliche Shackleton Range.

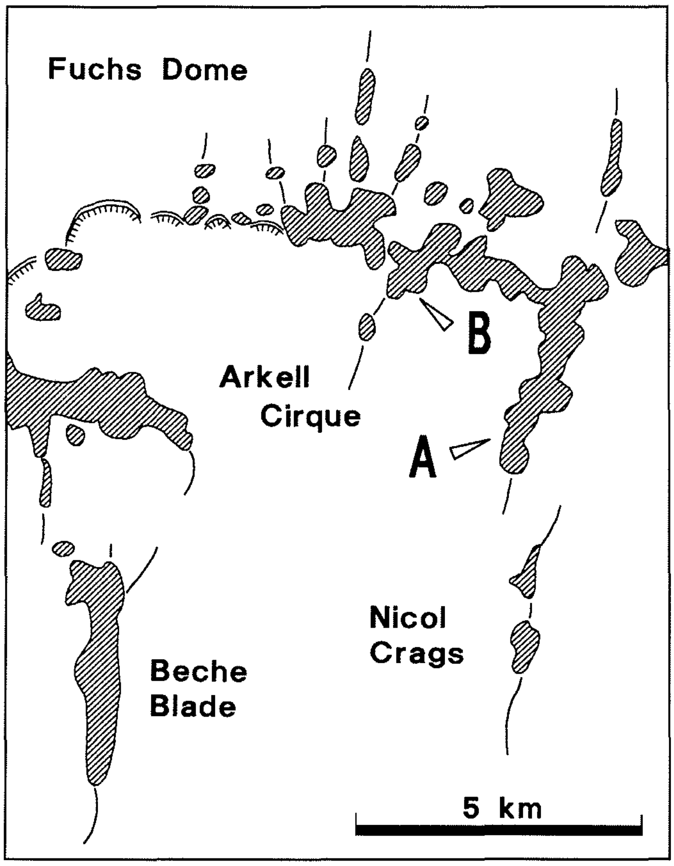

Fig. 10: Outcrops „A" and „B" in the Arkell Cirque, Read Mountains, southern Shackleton Range (see Fig. 2 for location).

Abb. 10: Aufschlüsse „A" und „B" innerhalb des Arkell Cirque, Read Mountains, südliche Shackleton Range (vergl. Abb. 2).

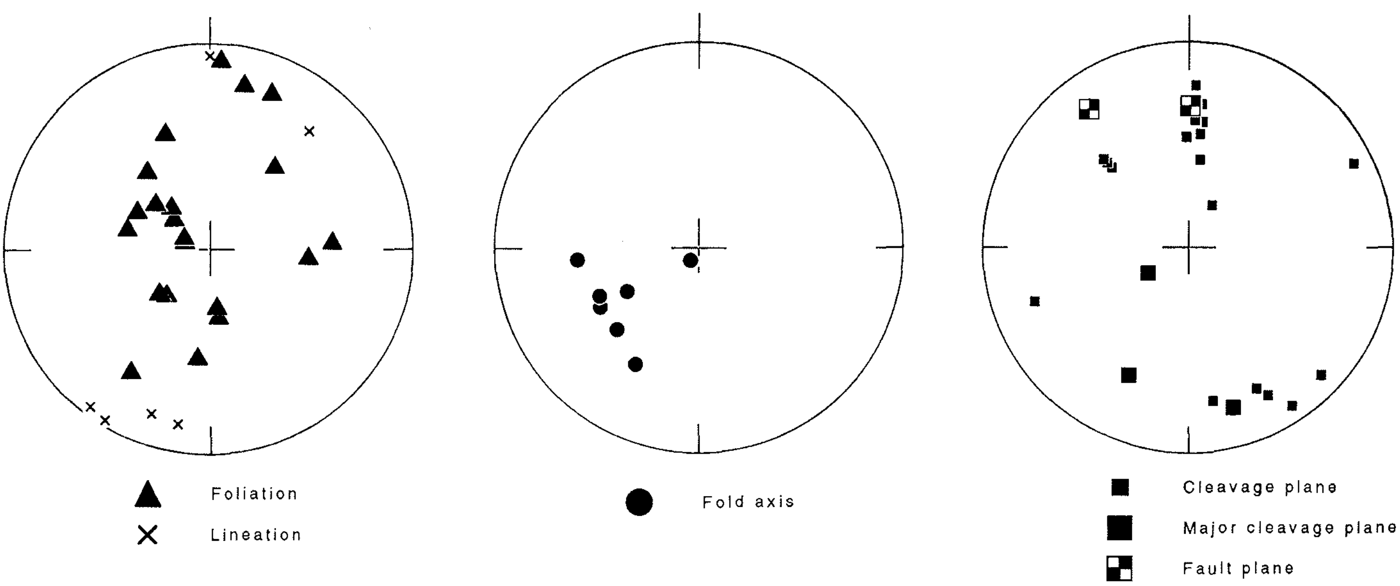

Fig. 9: Schmidt net projection of ductile and brittle deformation structures in Read Group metamorphics at Beche Blade, Read Mountains, southern Shackleton Range.

Abb. 9: Darstellung duktiler und bruchhafter Deformationsgefüge innerhalb der Read Group im Schmidt'schen Netz; Beche Blade, Read Mountains, südliche Shackleton Range.

lations on a mm scale run E-W. Pronounced cleavage is related to strain concentration at the margins of the rigid granitic body (Fig. 11). The SW-dipping planes resemble small reverse faults, whereas those which dip steeply W to NW represent dextral strike-slip faults parallel to the pegmatites. The granite is crossed by an E-W-striking, subvertical shear zone with N vergency. A NW-dipping, brecciated zone 20 cm wide contains fist-size granite fragments. Selective brecciation of individual layers indicates a high fluid content during this stage.

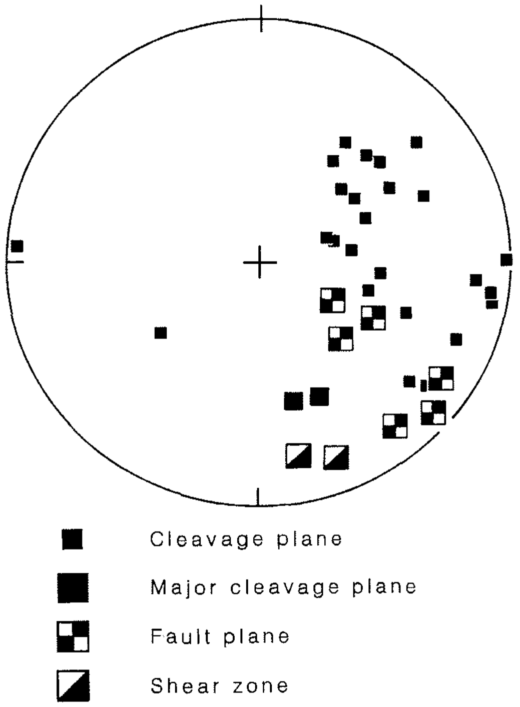

Fig. 11: Schmidt net projection of brittle deformation structures in Read Group metamorphics and granite; SE corner of Arkell Cirque (Fig. 10 „A"), Read Mountains, southern Shackleton Range.

Abb. 11: Darstellung bruchhafter Deformationsgefüge innerhalb der Read Group-Metamorhite und einer granitischen Intrusion im Schmidt'schen Netz; östlicher Arkell Cirque (Aufschluß „A" in Abb. 10), Read Mountains, südliche Shackleton Range.

Further north (Fig. 10"B"), biotite schists, hornblende schists, amphibolites, and granitic gneisses are interlayered on a scale of several cm to dm. Foliation planes are defined by the orientation of biotite and amphiboles. Competent quartzofeldspathic layers between easily deformable schists are affected by boudinage within a S-vergent rotational deformation regime (Figs. 12 and 13).

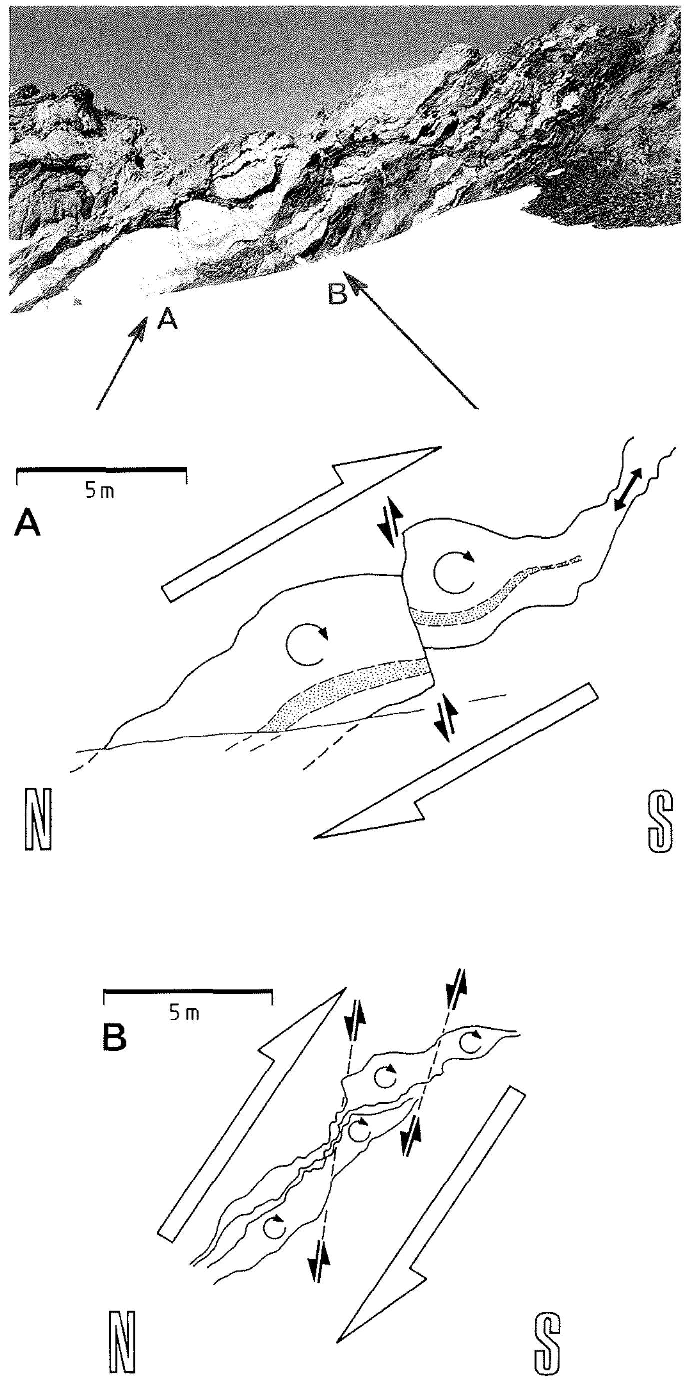

Fig. 12: Rotational boudinage of Read Group metamorphics associated with southward thrusting; varying types of boudinage and orientations of secondary shear planes, depending on thickness of competent layer (for Schmidt net projection of deformation structures, see Fig. 12); E margin of Arkell Cirque (Fig. 10 „A"), Read Mountains, southern Shackleton Range.

Abb. 12: Durch südwärts gerichtete Aufschiebung erzeugte rotationale Boudins innerhalb der Metamorphite der Read Group. Je nach Mächtigkeit der kompetenten Lage variieren der Typ der Boudinage und die Orientierung sekundärer Scherflächen (vergl. Abb. 12); östlicher Arkell Cirque (Aufschluß „A" in Abb. 10), Read Mountains, südliche Shackleton Range.

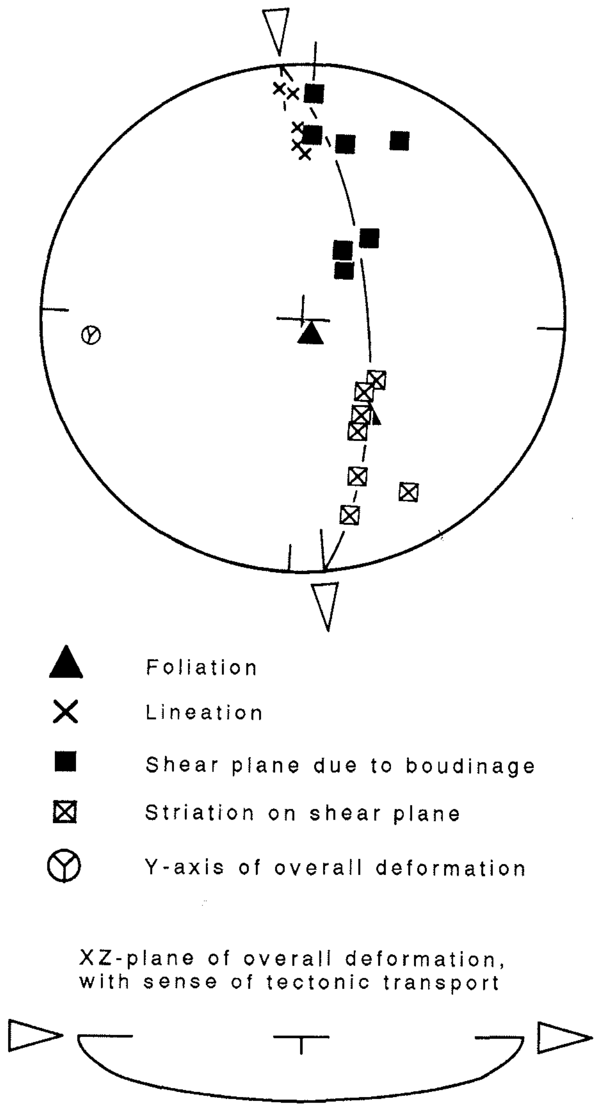

Fig. 13: Schmidt net projection of ductile deformation structures in Read Group metamorphics (shown in Fig. 11); E margin of Arkell Cirque (Fig. 10 „A"), Read Mountains, southern Shackleton Range.

Abb. 13: Darstellung der in Abb. 11 gezeigten tektonischen Gefüge im Schmidt'schen Netz; östlicher Arkell Cirque (Aufschluß „A" in Abb. 10), Read Mountains, südliche Shackleton Range.

2.2.4 Mount Wegener

On the NW spur of Mount Wegener, weathered granitic rocks of the Read Group are overlain by Watts Needle Formation sediments (Fig. 14). Violet-brown schists with variable thicknesses up to about 1 m occur at the boundary between these major units. They have been identified as remnants of a palaeosoil (Paech et al. 1987, Buggisch et al. 1990, 1994a). The basal sandstone layers of the Watts Needle Formation include granitic clasts several cm in diameter. Both the basement rocks and the sediments are cut by brittle fractures nearly perpendicular to the south-dipping unit boundary (Fig. 15).

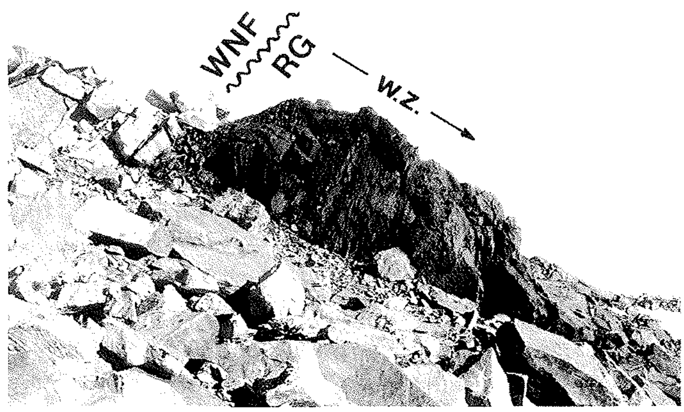

Fig. 14: Unconformity between Read Group (RG) granite and Watts Needle Formation (WNF) sandstone; weathering zone (w.z.) between the ancient land surface and the unmodified granitic basement (note the gradual change from dark, schistose weathering products to grey, massive granite); height of section roughly 5-7 m (perpendicular to planar fabric); south to the left; NW spur of Mount Wegener, Read Mountains, southern Shackleton Range.

Abb. 14: Diskordanz zwischen der Read Group (RG), und dem basalen Sandstein der Watts Needle Formation (WNF). Von der ehemaligen Landoberfläche ausgehende, in das Grundgebirge eingreifende Verwitterungszone (w.z. - beachte den graduellen Übergang von dunklen, schiefrigblättrigen Verwitterungsprodukten zu intaktem, grauem Granit). Aufschlußhöhe senkrecht zum Lagenbau ca. 5-7 m, Süden links. NW-Sporn von Mount Wegener, Read Mountains, südliche Shackleton Range.

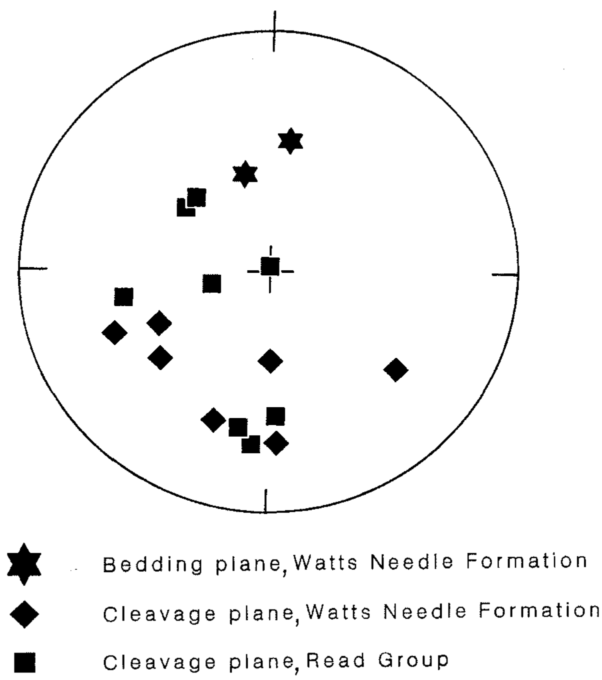

Fig. 15: Schmidt net projection of Watts Needle Formation sedimentary bedding and cleavage planes in both Read Group basement and sedimentary cover; NW spur of Mount Wegener, Read Mountains, southern Shackleton Range.

Abb. 15: Sedimentäre Schichtung (Watts Needle Formation), und Kluftflächen (Watts Needle Formation, Read Group) im Schmidt'schen Netz; NW-Sporn von Mount Wegener, Read Mountains, südliche Shackleton Range.

2.2.5 Gora Rudachenka

Gora Rudachenka consists of biotitic and amphibolitic schists in the north, and chiefly granitic gneisses in the southern part. The occurrence of migmatites, as indicated in figures by HOFMANN & PAECH (1983: 184) and PAECH (1985: 313, cross section 1), could not be confirmed. Porphyritic granites similar to the rocks at the NE corner of Beche Blade were found in the centre of the summit plateau of Gora Rudachenka. Both foliation and lineation are generally inclined to the north. Since folds are almost completely lacking, an interpretation as „b-lineation“ (HOFMANN & PAECH 1983) seems to be very disputable and contradicts the situation in most other outcrops. Feldspars within the porphyritic granites are usually randomly oriented. In a mylonitic shear zone, however, rounded relics of large feldspars show pronounced alignment parallel to the vector of tectonic movement (Fig. 16).

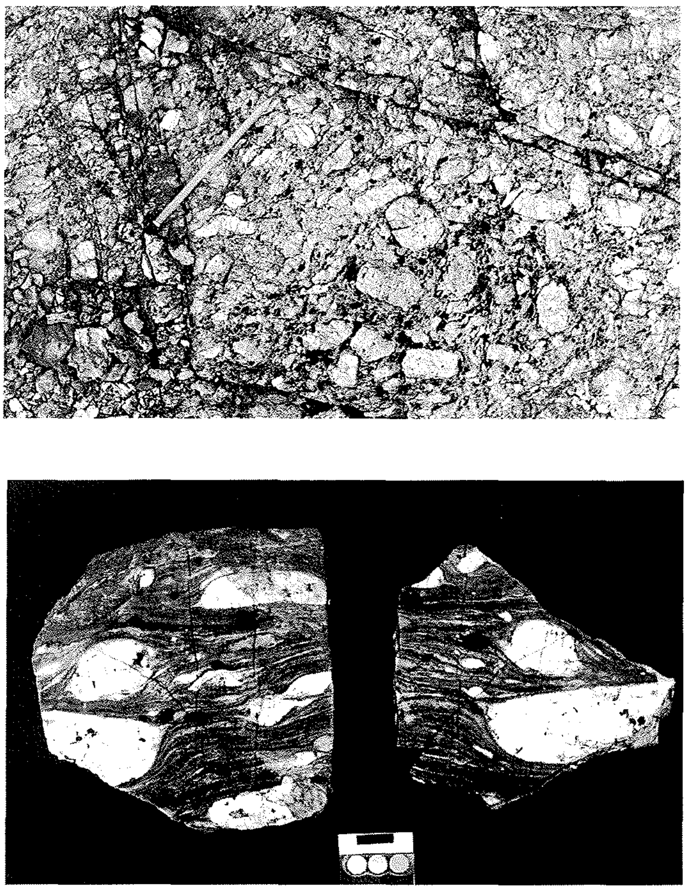

Fig. 16: Porphyritic granite on summit plateau of Gora Rudachenka, Read Mountains, southern Shackleton Range. Top: undeformed rock with large, randomly oriented feldspars. Length of pencil is about 15 cm. Bottom: Mylonite derived from porphyritic granite. Rounded feldspars have been rotated into the mylonitic foliation. Dark spots are relics of hornblende crystals. Scale bar= 1 cm.

Abb. 16: Porphyritischer Granit auf dem Gipfel-Plateau von Gora Rudachenka, Read Mountains, südliche Shackleton Range. Oben = ursprüngliches Gestein mit großen, unregelmäßig orientierten Feldspäten; Länge des Stiftes 15 cm. Unten = aus dem porphyritischen Granit hervorgegangener Mylonit. Die Feldspäte wurden abgerundet und sind in die mylonitische Schieferung einrotiert. Dunkle Flecken sind Relikte von Hornblende-Kristallen. Maßstab = 1 cm.

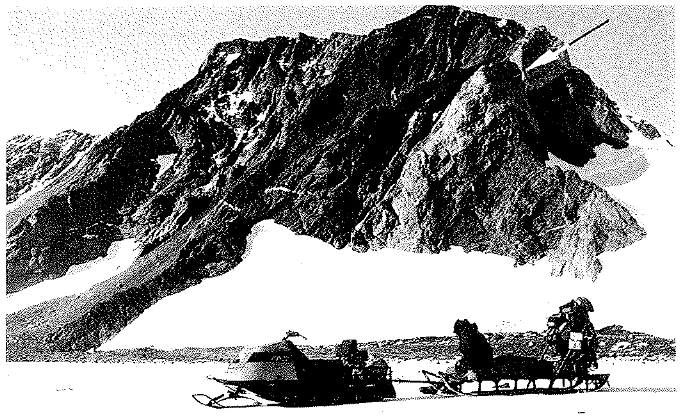

Fig. 17: View of the W-SW face of Gora Rudachenka, Read Mountains, southern Shackleton Range; arrow marks one of several N-S-striking, subvertical fault planes (see text).

Abb. 17: Blick auf die W-SW-Wand der Gora Rudachenka, Read Mountains, südliche Shackleton Range. Der Pfeil markiert eine in N-S-Richtung streichende, subvertikale Störungsfläche.

Thrust planes showing northward tectonic transport, as demonstrated by PAECH (1985: 313), were not confirmed during the GEISHA expedition. The apparent offset of the overlying rocks seen on the west face of Gora Rudachenka results from subvertical N-S-striking fault planes, i.e. roughly parallel to the rock face (Fig. 17). The geometry indicates that sinistral strike slip and/or normal faulting with downthrow on the west side must have taken place on these faults.

2.2.6 Outcrop SSW Flett Crags

Whereas the Mount Wegener Formation crops out on the ice-free ridge of Flett Crags, the crest some 100 m further SSW (USGS map, height 1749) consists of a strongly weathered gneiss with large, broken feldspars. This was probably derived from a rock similar to the porphyritic granites at Beche Blade and Gora Rudachenka. Densely packed feldspar „augen“ - in fact made up of several rotated fragments of larger crystals - lie with their longest dimension within the N-dipping planar fabric (Figs. 18 and 19). A NNE-plunging lineation results from the orientation of the feldspar aggregates, as well as from elongated quartz grains. Depending on the crystallographically defined primary orientation of internal shear planes with respect to the axes of deformation, the feldspar fragments rotate either synthetically or antithetically. Careful examination of shear sense indicators yields a N to S transport of the overlying rocks. Since the Mount Wegener Formation crops out only a few 100 m further north, the shear fabrics are most probably due to overthrusting of the Read Nappe (for fabrics within the basal part of the Mount Wegener Group, see KLEINSCHMIDT 1989, BUGGISCH et al. 1990, 1994a).

2.2.7 Hatch Plain

The E face of a NNE-SSW-trending ridge in the western part of the Hatch Plain (USGS map, height 1321) was examined

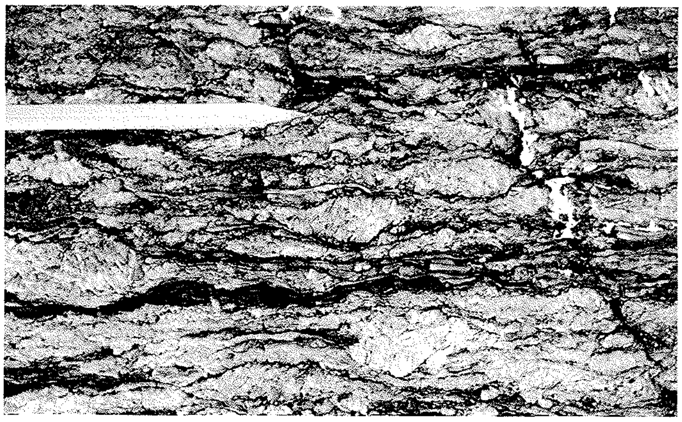

Fig. 18: Granitic gneiss from outcrop SSW of Flett Crags in the Read Mountains, southern Shackleton Range; the fracturing of feldspar and biotite foliation are due to southward thrusting (top to the left in this view).

Abb. 18: Granitischer Gneis in einem Aufschluß SSW Flett Crags in den Read Mountains, südliche Shackleton Range. Südwärts gerichtete Aufschiebung (in dieser Ansicht Rotation entgegen dem Uhrzeigersinn) führt zum Zerbrechen der Feldspäte und zur Anlage biotit-reicher Schieferungsflächen.

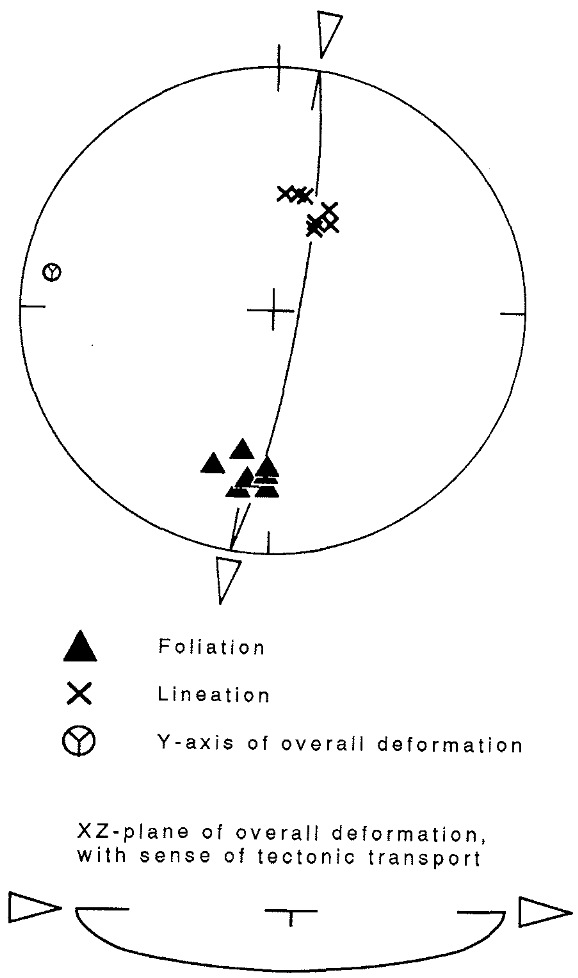

Fig. 19: Schmidt net projection of deformation structures in sheared porphyritic granite; SSW part of Flett Crags, Read Mountains, southern Shackleton Range.

Abb. 19: Darstellung der Deformationsgefüge innerhalb des tektonisch zerscherten porphyritischen Granits SSW Flett Crags im Schmidt'schen Netz; Read Mountains, südliche Shackleton Range.

during the GEISHA expedition. For detailed petrographic descriptions the reader is referred to SCHUBERT & OLESCH (in press).

The southern part of the outcrop is crossed by a WNW-ESE-striking, subvertical fault zone, which appears morphologically as a steep couloir. Finely laminated schists within the shear zone contrast with the compact gneisses on both sides. Rocks further S show two sets of cleavage planes. One system follows the orientation of the master fault and is marked by small aplitic veins. A shear plane dipping gently WSW terminates in the large fault zone; its sense of tectonic offset remains undefined. Another shear plane further north, which is inclined ESE, shows SE downthrow of the overlying rocks.

In a stereographic plot, poles of foliation planes from Hatch Plain and a small outcrop further NW lie on a great circle with a SE-plunging axis (Fig. 20). Thus, NW-SE lineations may represent b-lineations, but no small-scale folds were observed (with wavelengths of a few dm to several m). In fact, asymmetric pressure shadows in oriented samples are evidence for a NW-SE orientation of the XZ-plane of ductile deformation. The parallelism of lineation and fold axes therefore seems rather coincidental.

2.2.8 Poldervaart Edge

Poldevaart Edge consists of a NNE-SSW-trending chain of isolated knolls covered with ice to the west, but forming cliffs several 10 m high on the E side. All outcrops show southerly dipping foliation planes and a lineation plunging S to E. Several subvertical fault planes strike parallel to the fault zone at Hatch Plain. They are N-dipping normal faults.

2.3 *Development and geometry of the so-called „Read Anticline"*

The orientation pattern of the syn-metamorphic foliation led previous authors to assume a large, E-W-striking antiform in the Read Mountains. However, since the original orientation of an old fabric usually cannot be reconstructed without knowledge of the geometry of younger structures, foliation planes are not necessarily a reliable source of information. In the Read Mountains, additional control is provided by the tilt of the Watts Needle Formation. The stromatolitic carbonates provide an excellent marker bed that was certainly horizontal during sedimentation. In the central Read Mountains (Watts Needle, Nicol Crags), they remained subhorizontal, but at Mount Wegener they dip due S at 40 - 50°. In the northern Read Mountains, rocks of the Watts Needle Formation are absent (BUGGISCH et al. 1994a). The N-dipping top of the basement represents a major tectonic shear zone that is thought to be equivalent to the concordant thrust plane between Watts Needle Formation and Mount Wegener Formation further south (ROLAND et al.1988, BUGGISCH et al.1990). As a matter of fact, the attitudes of the planes mentioned above indicate late folding on a subhorizontal, E-W axis (Fig. 21), which confirms the somewhat tentative approach of previous authors.

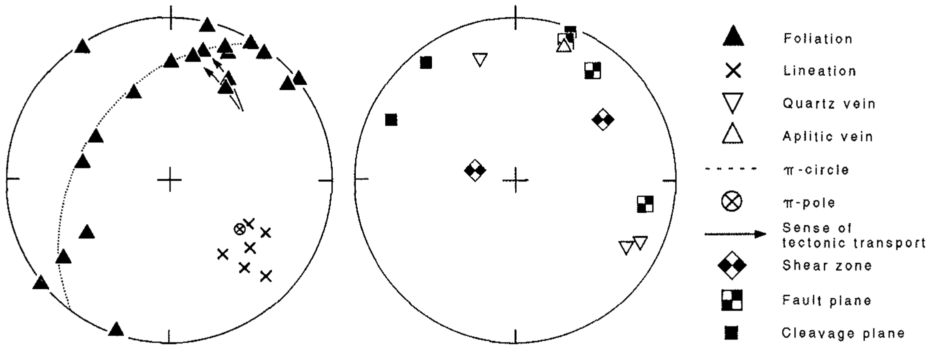

Fig. 20: Schmidt net projection of ductile and brittle deformation structures in Read Group metamorphics on Hatch Plain, Read Mountains, southern Shackleton Range.

Abb. 20: Darstellung duktiler und bruchhafter Deformationsgefüge innerhalb der Read Group im Schmidt'schen Netz; Hatch Plain, Read Mountains, südliche Shackleton Range.

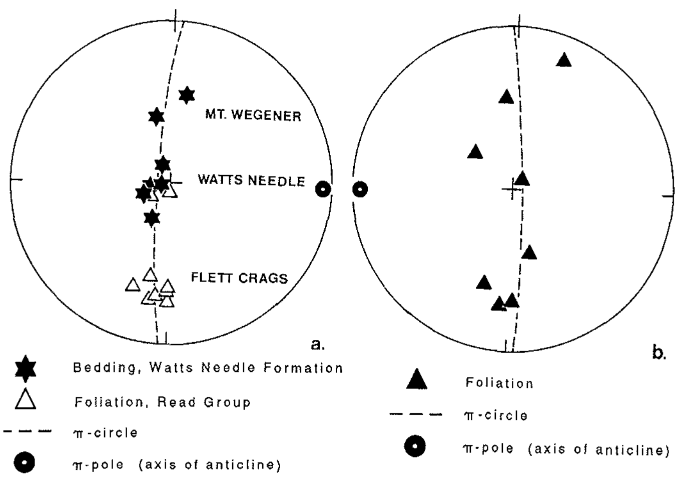

Fig. 21: Reconstruction of the „Read Anticline" axis (Read Mountains, southern Shackleton Range); (a) from the orientation of originally subhorizontal planes and (b) from the statistic maxima of foliation measurements in several outcrops.

Abb. 21: Rekonstruktion der Achse der „Read-Antikline" (Read Mountains, südliche Shackleton Range): (a) aus der Verkippung ursprünglich horizontal liegender Gefüge, und (b) aus den statistischen Maxima der Schieferungsflächen in diversen Aufschlüssen.

The existence of large-scale tilting in the Read Mountains is obvious, but true-scale N-S sections (i.e. perpendicular to the axis of rotation) reveal that the former concept of a single anticline is too simple. In the east, the fold axis is in the gap between Gora Rudachenka and Mount Wegener. In the central Read Mountains (between Watts Needle and Nicol Crags), the anticlinal axis seems to be several km further south (Fig. 22). Three different explanations are possible: (i) Doming actually did produce one single anticline, but the central Read Mountains have been subsequently displaced further S. (ii) The apparent E-W axis of rotation does not result from large-scale folding, but from differential rotation of independent blocks. (iii) There is not one major anticline, but two anticlines and one syncline due to large-scale upright folding.

The first two models necessitate the assumption of fault planes across the E-W axis of rotation, but up to now very few strike-slip planes are known (e.g. at Gora Rudachenka) and even these are doubtful. The third model well explains the present large-scale geometric arrangement, even though no corresponding folds have been found in outcrop or on hand-specimen scale.

A similar large-scale E-W fold is known from Stephenson Bastion (CLARKSON 1982a, BRAUN et al. 1988). By assuming a position in the hinge area of a major upright fold, the somewhat peculiar, north-vergent „reverse faults" within the Mount Wegener Nappe at Mount Wegener (BUGGISCH et al. 1994a) may be explained as „usual" synthetic shear zones. Since not only the sole thrust plane of the Mount Wegener Formation, but (to our present knowledge) the whole nappe unit has been affected by late tectonic tilting, the area E of the Read Window (Lapworth Cirque, Goldschmidt Cirque, Trueman Terraces) is probably the best region to verify the assumption of multiple upright folds.

2.4 *Reconstruction of kinematic directions*

By using the rotation axis calculated above, and the outcrop-specific parameters listed in Table 1, it is now possible to reconstruct the situation prior to the very last tilting event, and to determine former kinematic directions (i.e. overall XZ-planes of deformation). Structures within the Watts Needle Formation, i.e. below the Mount Wegener Nappe (classified as „type C" in Tab. 1), are related to overthrusting by the allochthonous Mount Wegener Formation. They indicate a NW to SE sense of tectonic transport (Figs. 23 and 24). This direction is slightly different from results by BUGGISCH et al. (1990, 1994a), who deduced N to S transport from deformation fabrics within the nappe. This discrepancy may have local reasons (e.g. mechanical influence of the allochthonous crystalline block on top of Watts Needle, or local ramp structures oblique to the direction of tectonic transport), but may characterize the overall kinematics of crustal deformation (e.g. a transpressional component of deformation).

2.5 *Tectonometamorphic evolution of the Read Mountains*

Five main phases of events in the Read Mountains can be distinguished:

- metamorphism and ductile deformation of the basement (Read Group);
- uplift, erosion and cooling of the basement, formation of a land surface with smooth morphology;
- subsidence of the crust, and sedimentation of the Watts Needle Formation;
- thrusting of the Mount Wegener Formation (Mount Wegener Nappe);

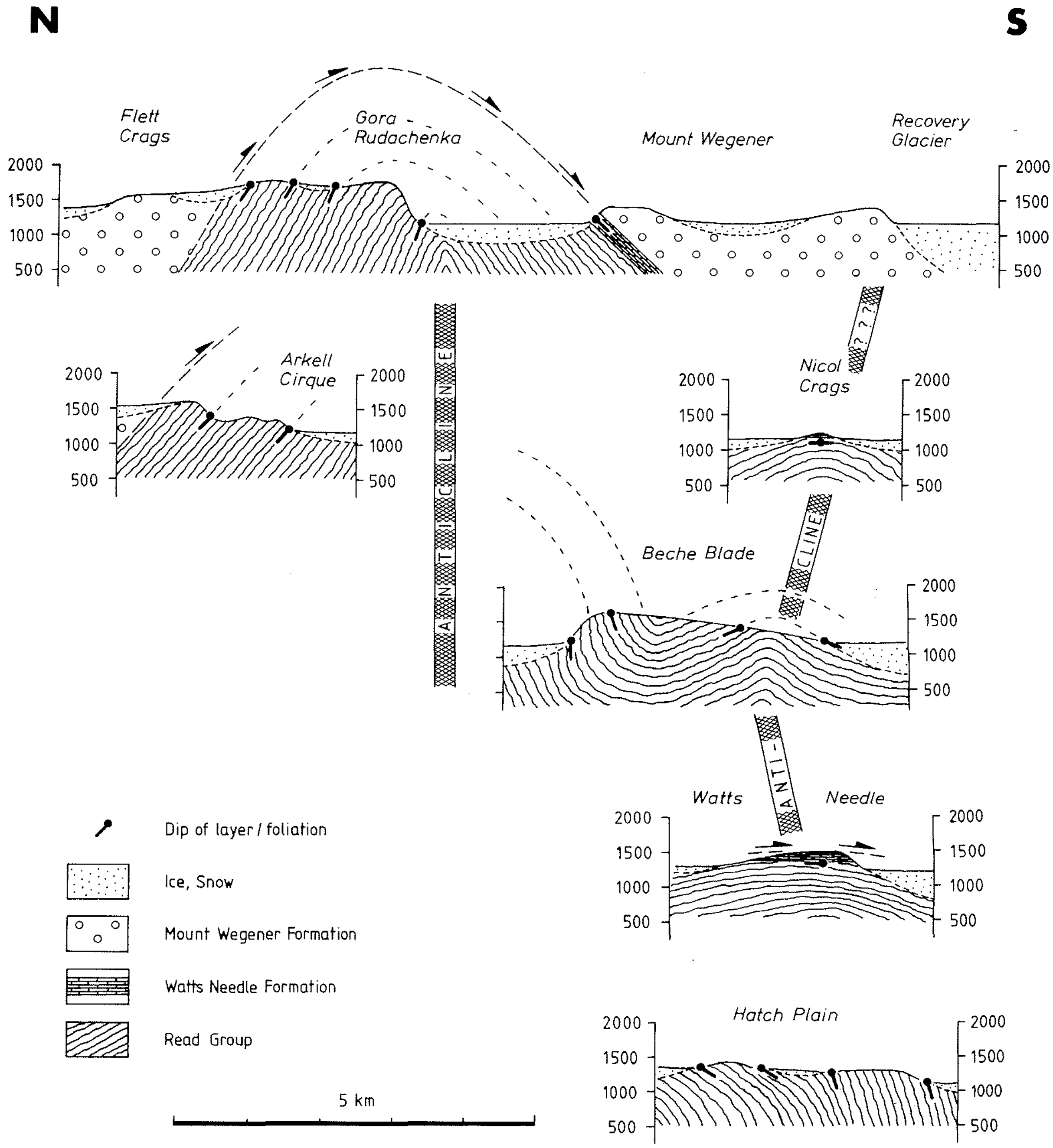

Fig. 22: Simplified true-scale N-S sections across the Read Mountains, southern Shackleton Range, showing large-scale Palaeozoic folding as interpreted from dip measurements of metamorphic foliation, unit boundaries, and sedimentary layering (no vertical exaggeration). Structures related to the preceeding Proterozoic tectono-metamorphism (i.e. local folds, intrusives etc.) not shown in detail. Vertical scale in meters a.s.l.

Abb. 22: Vereinfachte, N-S gerichtete Profilschnitte durch die Read Mountains, südliche Shackleton Range (nicht überhöht). Die heutige Orientierung der Schieferungsflächen, der stratigraphischen Grenzen, und der sedimentären Schichtflächen kann als Resultat einer großmaßstäblichen paläozoischen Verfaltung interpretiert werden. Ältere proterozoische Strukturen (lokale Falten, Intrusionen) sind hier nicht im Detail gezeigt. Vertikaler Maßstab in Metern über NN.

– final uplift and erosion (recent morphology).

Elaborating on this framework by adding some details described in section 2.2, an attempt will be made to characterize the regional behaviour of the crust, as well as to narrow down the absolute time range for some important phases of the geological evolution.

The pre-metamorphic source rocks of the Read Group remain subject to speculation. Neither petrographic studies nor radiometric dating present convincing proof of early Proterozoic or even Archean events. Concordant granitic and pegmatitic layers, and hornblende-rich mafic rocks may point to early intrusive activity, which is possibly represented by a single, unpublished Sm-Nd age of 1960-2000 Ma (Belyatsky pers. comm.).

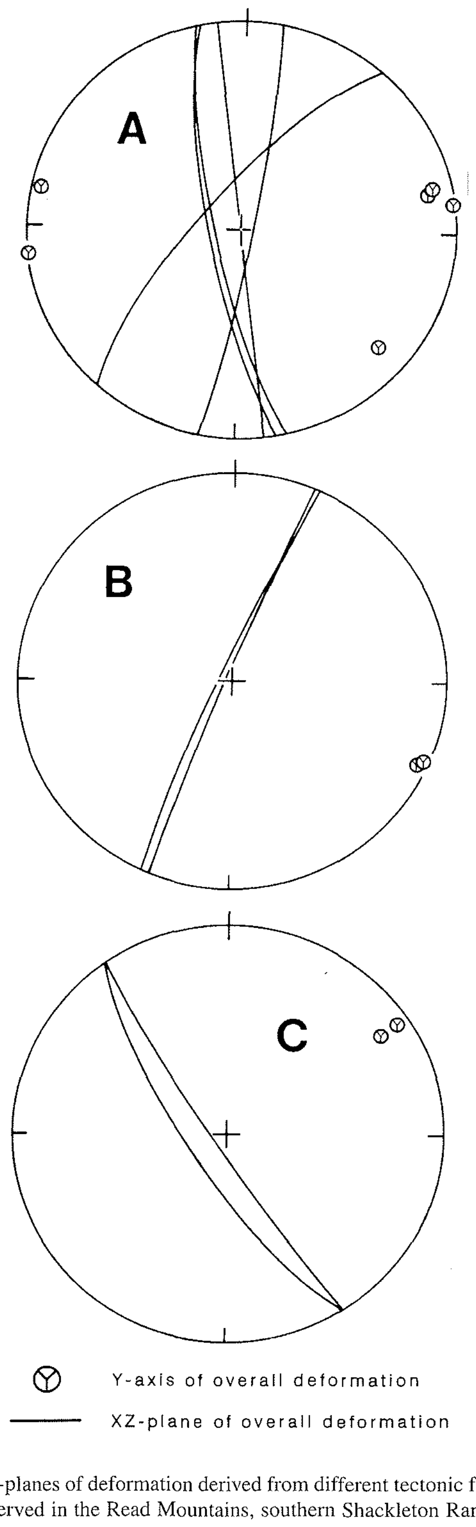

Fig. 23: XZ-planes of deformation derived from different tectonic features (A, B & C) observed in the Read Mountains, southern Shackleton Range; shown in original orientation, i.e. after elimination of late anticlinal folding (for further information, see text and Tab. 1).

Abb. 23: XZ-Ebenen der Deformation in der südlichen Shackleton Range, abgeleitet aus unterschiedlichen Gefügetypen (s. Tab. 1, Typen „A" bis „C"). Darstellung im Schmidt'schen Netz in ursprünglicher Orientierung, d.h. nach Rück-Rotation der späten Verfaltung, die zur sog. „Read-Antikline" führte (weitere Informationen s. Text).

Metamorphism in the Read Mountains reached upper amphibolite facies (Clarkson 1982a), with P-T conditions estimated from metamorphic mineral parageneses at about 600 °C and 4.5-6 kbar. These values are widely confirmed by microanalytical investigations (Olesch 1991), except some questionable higher pressure data resulting from ternary feldspar thermobarometry (Schulze 1989). Prograde minerals grew parallel to the compositional layering and created a distinct planar fabric. Non-rotational boudins suggest syn-metamorphic N-S extension, which is supported by symmetric grain orientation fabrics due to flattening strain. Tectonic thinning of the whole crust may be deduced from the geothermal gradient, which exceeds normal Proterozoic conditions (Lambert 1983).

Pegmatitic veins and agmatites crosscutting the main metamorphic fabric are related to granitic intrusions encountered in the area between Watts Needle and The Ark, and in the southeastern part of the Arkell Cirque. Biotite growth parallel to the foliation planes in surrounding metamorphics, narrow reaction margins, and similar grain sizes in palaeosome and neosome indicate still rather high basement temperatures during intrusion. Whole-rock dating of the granites yielded ages of about 1800 Ma (Pankhurst et al. 1983). The formation of the first, intrafolial folds may indicate a change from crustal extension to crustal compression.

Southward thrusting commenced under ductile conditions and led to rotational boudinage in the Arkell Cirque. New, retrograde minerals grew oriented within the previous plane of foliation. Although Pankhurst et al. (1983) referred to a Rb-Sr whole-rock determination of 1599 ±38 Ma as „metamorphic age"; this date in fact represents closure of the isotope system, i.e. roughly the time when these rotational structures formed. This conclusion corresponds well with biotite ages between 1659 and 1530 Ma (Buggisch et al. 1994a).

Porphyritic granites with large feldspars are widespread in the basement rocks of the Read Mountains (e.g. Beche Blade, SSW Flett Crags, Gora Rudachenka, ? Watts Needle summit). In contrast to the fine-grained syn-metamorphic granites, they postdate pervasive ductile tectonic deformation. For the porphyritic granite on the NE side of Beche Blade, Hofmann et al. (1980) obtained a K-Ar age of 1401 ±70 Ma. Coarse-grained granitic rocks from Strachey Stump (E of Gora Rudachenka) have been dated at 1487 and 1424 Ma. Granodiorites with similar Rb-Sr ages of 1454 ±60 Ma (Pankhurst et al.1983; recalculated from a measurement by Rex 1972) were not investigated during this study. Palaeostress calculations on shear zones at Gora Rudachenka and Watts Needle suggest NW-SE tectonic compression for this time.

Right-angled kink folds with wide-spaced axial plane cleavages, and gentle open warping on N-S to NW-SE axes terminated the Proterozoic cycle of metamorphism and deformation. NE-SW compression of the crust, as deduced from the orientation of fold axes, possibly also produced E- to NE-vergent reverse faults in the Arkell Cirque.

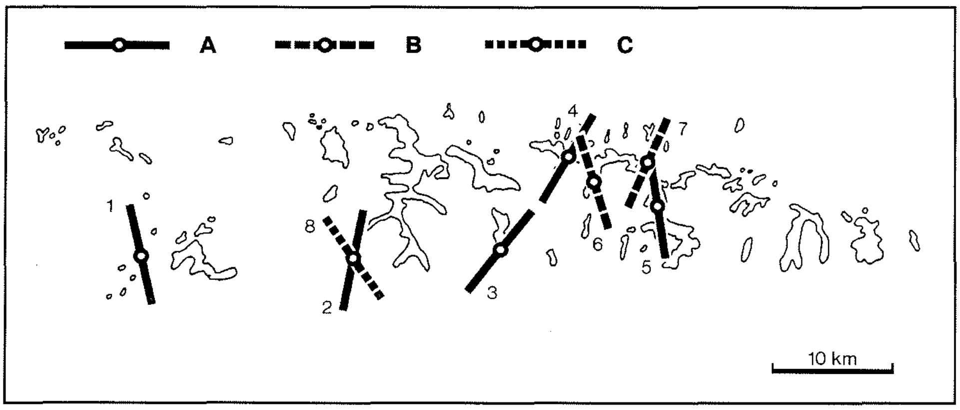

Fig. 24: Regional pattern of deformational XZ-planes in the Read Mountains, southern Shackleton Range (see also stereoplots in Fig. 23). Shown are lines of intersection of XZ-planes with the horizontal plane. (For meaning of numbers 1-8 and letters A-C, refer to Table 1; for location, see Figs. 1 and 2).

Abb. 24: Lokale Lage der XZ-Ebene der Deformation (Schnittspur mit der Horizontalen); Read Mountains, südliche Shackleton Range (vergl. Diagramme in Abb. 23). Referenz-Ziffern und Typisierung „A" bis „C" beziehen sich auf Tab. 1; geographischer Rahmen s. Abb. 1 und 2.

Type	XZ-plane of deformation constructed from...	Ref. No.	Locality	Rotation
		1	Poldervaart Edge	+45°
		2	Watts Needle	± 0°
A	...synsedimentary foliation planes and lineations	3	Beche Blade (S)	+20°
		4	Arkell Cirque (NW)	–40°
		5	Gora Rudachenka (SW)	–60°
	...retrograde shear zones,	6	Arkell Cirque (NE)	–40°
B	lineations and secondary shear planes	7	SSW Flett Crags	–60°
C	...thrust-induced folds and deflected foliation planes	8	Watts Needle	± 0°

Tab. 1: Data for the reconstruction of the original (prior to late folding) deformational XZ-planes in the Read Mountains, southern Shackleton Range. Types A, B, C refer to different tectonic features used as marker horizons (see Figs. 23 and 24). Last column gives rotation angles necessary to eliminate the effect of late folding (rotation axes derived from diagrams in Fig. 21). Positive values = marker horizon dips S today; negative values = marker horizon dips N today. Locality numbers as in Fig. 24.

Tab. 1: Basisdaten für die Rekonstruktion der Deformation in ihrer ursprünglichen Lage, d.h. vor der späten Verfaltung (Read Mountains, südliche Shackleton Range). Die Typen „A" bis „C" charakterisieren verschiedene, als Markierungsebene für die ursprüngliche Horizontale benutzte Gefüge (s. Abb. 23 und 24). Die letzte Spalte enthält den Winkelbetrag für deren Rück-Rotation um die in Abb. 21 ermittelte Faltenachse (positive Werte = Gefüge fällt heute nach Süden ein; negative Werte = heutiges Einfallen des Gefüges nach Norden).

Uplift, cooling and erosion of the Read Group led to the paleorelief on which the Watts Needle Formation was deposited. Acritarchs from the weathering horizon, which are preserved in some places, have been assigned to the upper Riphean, i.e. the Late Proterozoic (WEBER 1991).

Sedimentation of the Watts Needle Formation occurred during the Eocambrian. Basal sandstones have been dated at 680 ±57 Ma (Rb-Sr), while pelitic rocks near the top yielded 584 ±41 Ma (BUGGISCH et al. 1994a). The stromatolites of the carbonate member of the Watts Needle Formation have been assigned to the Late Precambrian (GOLOVANOV et al. 1979).

Overthrusting of the Mount Wegener Nappe, i.e. the Mount Wegener Formation and some crystalline rocks dragged along in the sole thrust, caused intense SE-verging deformation in the upper part of the Watts Needle Formation and local southward shearing within the basement (e.g. outcrop SSW of Flett Crags). The allochthonous Mount Wegener Formation suffered syn-tectonic greenschist facies metamorphism (BUGGISCH et al. 1994a). Syn-tectonic to late-tectonic mica has K-Ar ages of roughly 490 Ma (BUGGISCH et al. 1990, 1994a). Thus, the emplacement of the Mount Wegener Nappe correlates with the Ross orogeny in the Transantarctic Mountains.

Tilting of the stacked rock units - probably due to large-scale folding - is the final act of deformation that has been directly observed in the Read Mountains. North-vergent reverse faults in the northern part of Beche Blade are in good agreement with the model of an upright double fold, because this region would be situated in the central, compressional zone of a synclinal fold.

For the age of latest uplift and erosion in the Read Mountains, unroofing of the basement in the central Read Mountains and creation of the „Read Window", there is only indirect evidence. According to BUGGISCH et al. (1994b), the Ordovician Blaiklock Glacier Group in the northern Shackleton Range contains erosional debris from a rising mountain belt (? Ross Orogen). The lack of Beacon Group sediments in the Shackleton Range may indicate that this area was subjected to uplift and erosion at least until the Palaeozoic/Mesozoic boundary. Fission track dating on apatites, commonly believed to indicate crossing of the 100 °C isotherm, yielded ages of 165 ±10 and 146 ±9 Ma (CLARKSON pers. comm.).

2.6 *Discussion*

The time of anticlinal doming in the Read Mountains relative to its metamorphic and intrusive history is a matter of controversy. HOFMANN & PAECH (1983) draw a direct connection between the rising anticline(s) and late-metamorphic intrusive activity (their Fig. 3, event „D2"), thereby postulating that this event took place at about 1400-1450 Ma (age of the youngest igneous rocks in the southern Shackleton Range). This hypothesis of early Late Proterozoic upwarping is in contradiction to the fact that tectonic tilting also affects the Watts Needle Formation, which is younger than about 680-580 Ma, and even the allochthonous Mount Wegener Formation, which was thrust as a nappe at about 490 Ma. To the author it therefore seems conclusive that doming (folding?) took place chiefly in Cambro-Ordovician times, i.e. syn-orogenic to late-orogenic with respect to the Ross event. Since Phanerozoic magmatism can be excluded at present for the southern Shackleton Range, a genetic relationship between granitic intrusions and updoming becomes irrelevant. For the same reason, the southern Shackleton Range cannot be interpreted as a „metamorphic core complex" comparable, for example, to the Cenozoic of North America. In addition, large-scale upright folding in the Read Mountains and other areas of the Shackleton Range indicates a compressional tectonic regime and not crustal thinning, which is a basic requirement for typical metamorphic core complexes (e.g. CONEY 1980, WERNICKE & BURCHFIEL 1982).

As has been shown above, the old land surface below the Watts Needle Formation cuts the basement at the level of amphibolite facies rocks, i.e. equivalent to an original depth of at least about 15 km, according to the results of geobarometry. The time interval of about 800 Ma between closure of the radiometric systems and deposition of sediment on the eroded basement is characterized by a complete lack of major tectonic structures and intrusive activity. Generally, an inversion from a long period of uniform uplift to slow subsidence at the Proterozoic/Palaeozoic boundary is typical for many cratons consolidated during the mid-Proterozoic, and is usually assigned to cooling of the crust (e.g. CONDIE 1989).

3. TECTONOMETAMORPHIC EVOLUTION OF THE NORTHERN HASKARD HIGHLANDS

3.1 *General outline*

In the area between Mount Provender, Mount Weston, and Mount Gass, MARSH (1983a) distinguished four lithological units: the Nostoc Lake Formation, the Mount Gass Formation, the Mount Weston Gneiss, and the Stratton Gneiss. Rocks of the Nostoc Lake Formation and Mount Gass Formation are supracrustal metasediments belonging to the recently defined Pioneers Group. They are distinguished on the basis of relative quantities of certain rock types, but as MARSH (1983 a) has already pointed out, they may represent a single, continuous succession. The genetic significance of the Mount Weston and Stratton gneisses is unclear. The present author's studies in the Haskard Highlands were concentrated on structural relationships between the various units and their internal tectonometamorphic history. Three areas were investigated in detail (see Fig. 25 - elevations from the International Map of the World, USSR, 1982):

Area 1: Heights 853, 850, and 822 between Mount Provender and Pratts Peak;
Area 2: Narrow crest leading from height 1039, N of Mount Weston, towards Pratts Peak;
Area 3: Ridge between Mount Weston and Mount Gass, including heights 847 and 888.

Areas 1 and 2 have been lithologically mapped at a scale of about 1: 10,000. Since at the time of the GEISHA expedition large-scale maps were not available, topographic features in Figs. 26, 30, 34 (and related figures) may be artificially distorted to a certain degree, but this will not affect the geological information. Petrographic descriptions of some rocks have been given by STEPHENSON (1966) and MARSH (1983a).

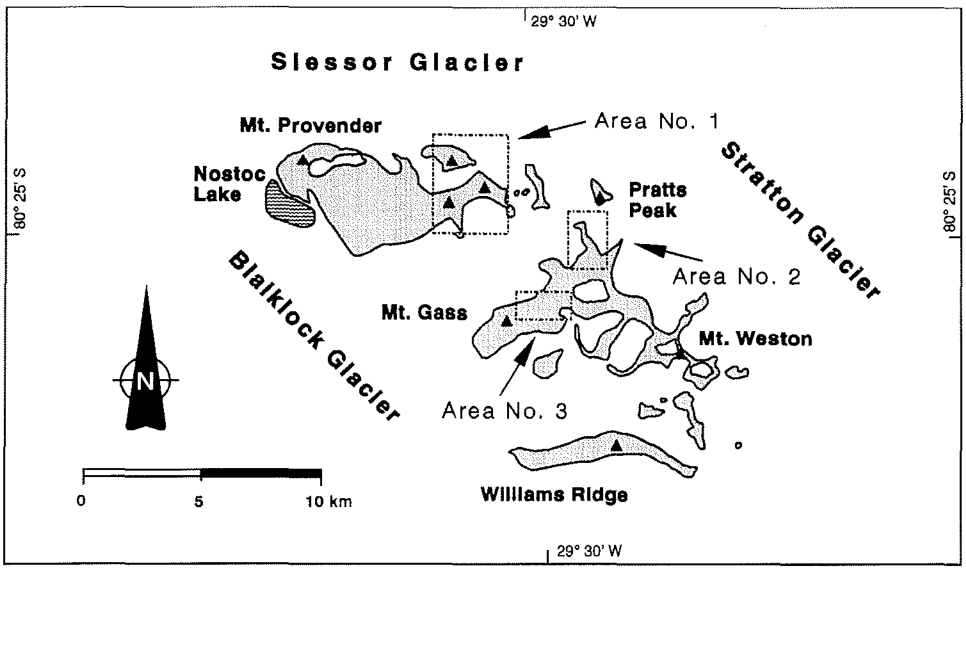

Fig. 25: Areas 1 to 3 in the Haskard Highlands of the northern Shackleton Range, in which detailed geological and structural mapping has been conducted (see also Fig. 1).

Abb. 25: Gebiete 1 bis 3 in den Haskard Highlands, nördliche Shackleton Range, in denen eine lithologische und strukturgeologische Kartierung erfolgte (geographischer Rahmen s. Abb. 1).

3.2 *Lithology and macroscopic structures*

3.2.1 Area east of Mount Provender (Area 1)

3.2.1.1 Lithology

The area east of Mount Provender consists of a series of carbonates, calc-silicates, quartz-rich gneisses, biotite metapelites with or without garnet, and subordinate amphibolites and garnet amphibolites (Fig. 26). Typical thicknesses of the layers range between several metres and a few tens of metres.

The general structure of the area is excellently marked by coarse-grained marble layers, which often occur in close association with thin layers of amphibolite (in particular at heights 850 and 822). Rocks on the northern side of height 853 contain pyroxene relics in a coarsely crystallized garnet amphibolite. Calc-silicate rocks have been mapped in a small area south of height 853. Thin layers of pure quartzite crop out in this area and also E of height 822. Garnet blasts in metapelitic rocks are remarkably „fresh", i.e. void of cracks and retrograde alteration. Violet-brown schists contain remarkable amounts of garnet and kyanite; the latter measure up to 1 cm in length. They grew parallel to the main schistosity, but within these planes the orientation of their long axes varies to a certain degree. Some gneisses contain relatively large, angular feldspar and quartz fragments, which sometimes form polycrystalline aggregates. Since these layers are intercalated with other metasediments, it is suspected that they represent metaconglomerates or non-tectonic metabreccias.

Quartz-rich granitic rocks on the eastern side of heights 850 and 822 and W of the latter have been described as „Stratton Gneiss" (Marsh 1983a). Biotite is concentrated in nebulous streaks along the margins of the intrusion, reminiscent of magmatic flow structures. A zone of agmatites 10-20 m wide in the northern part of the outcrop area marks the contact of the Stratton Gneiss with the surrounding metasediments. It is not yet certain whether „several discrete belts of Stratton Gneiss" within the metasediments (Marsh 1983a) are connected with the granitic intrusion described above. These concordant layers may represent quartzites of sedimentary origin, with very minor additions of feldspar and biotite.

The south spur of height 853 consists of an augen gneiss with large isolated feldspars set in a brown-red, fine-grained matrix. In the northern part, feldspar is subidiomorphic or slightly rounded, with mean lengths of 2-3 cm. The degree of tectonic flattening increases towards the south. Shear zones are marked by an intense schistosity and extreme ellipticity of feldspar lenses (aspect ratios exceeding 10). Flattened dark xenoliths containing garnet and with narrow feldspar rims point to a igneous nature of the augen gneiss.

3.2.1.2 Structure

The general strike of the metasediments varies between NNW-SSE and W-E (see also Marsh 1983a: Fig. 2, zone 2). Foliation planes are mostly parallel to the lithological boundaries. Lineations plunge west at an average of about 30° (Figs. 27, 28). Both foliation and lineation are caused either by oriented growth of lamellar or prismatic minerals (mica, hornblende, actinolite, kyanite, and sometimes feldspar) or by minerals and mineral aggregates that were elongated and/or flattened during ductile deformation. These fabrics represent the oldest macroscopic structures (Fig. 28, stereoplots I, II, and III).

Geological mapping and the construction of cross sections revealed large-scale folds with amplitudes of several 100 m up to about 1 km (Fig. 29). Subordinate folds with short limbs of about 10 m, which are excellently exposed on the N side of height 853, have W to SW-plunging axes (Fig. 28, stereoplots I, II, and III). Generally their axial planes are steep to vertical. The fact that the axial plane of a fold seen at height 850 is gently dipping may be due to the presence of the rigid granitic body further E. The folds, as well as steep, E-W-striking thrust planes around height 822, indicate an appreciable amount of crustal shortening.

Tight to isoclinal folds on a scale of several dm to about 1 m have axial planes parallel to the foliation. From field observations, their axes seem to be co-linear with the axes of the large upright folds, as well as with the lineation. On the stereoplots, however, the small folds appear to have been rotated anticlockwise by about 20° relative to the lineation. Assuming tectonic transport perpendicular to the fold axes, long versus short limb relations indicate southward tectonic transport. Since this observation is valid independent of the relative position of the small folds within the major folds, an interpretation as parasitic folds is obsolete. The isoclinal folds obviously represent an intermediate generation (Fig. 28, stereoplots I, II, and III).

3.2.2 Area between Mount Weston and Pratts Peak (Area 2)

3.2.2.1 Lithology

Marsh (1983a) introduced the term „Mount Weston Gneiss" for the rocks north of Mount Weston and in the summit area of height 1039 (Fig. 30). Flattened quartz and/or feldspar lenses are enveloped in anastomosing silver-grey sheets, which serve as mechanical separation planes. Garnets up to 2 cm in diameter are rich in inclusions. The proportion of white mica increases from the Mount Weston massif towards Pratts Peak and Mount Gass. Streaks of mica on the foliation planes and pressure shadows around garnet, magnetite, and other rigid clasts have the same orientation.

North and structurally above the Mount Weston Gneiss, there is a layer of yellow to white quartzite about 200 m thick which shows a streaky lineation even more pronounced than that in the Mount Weston Gneiss. The proportion of mica increases and the rocks become more schistose northward. The lower part of

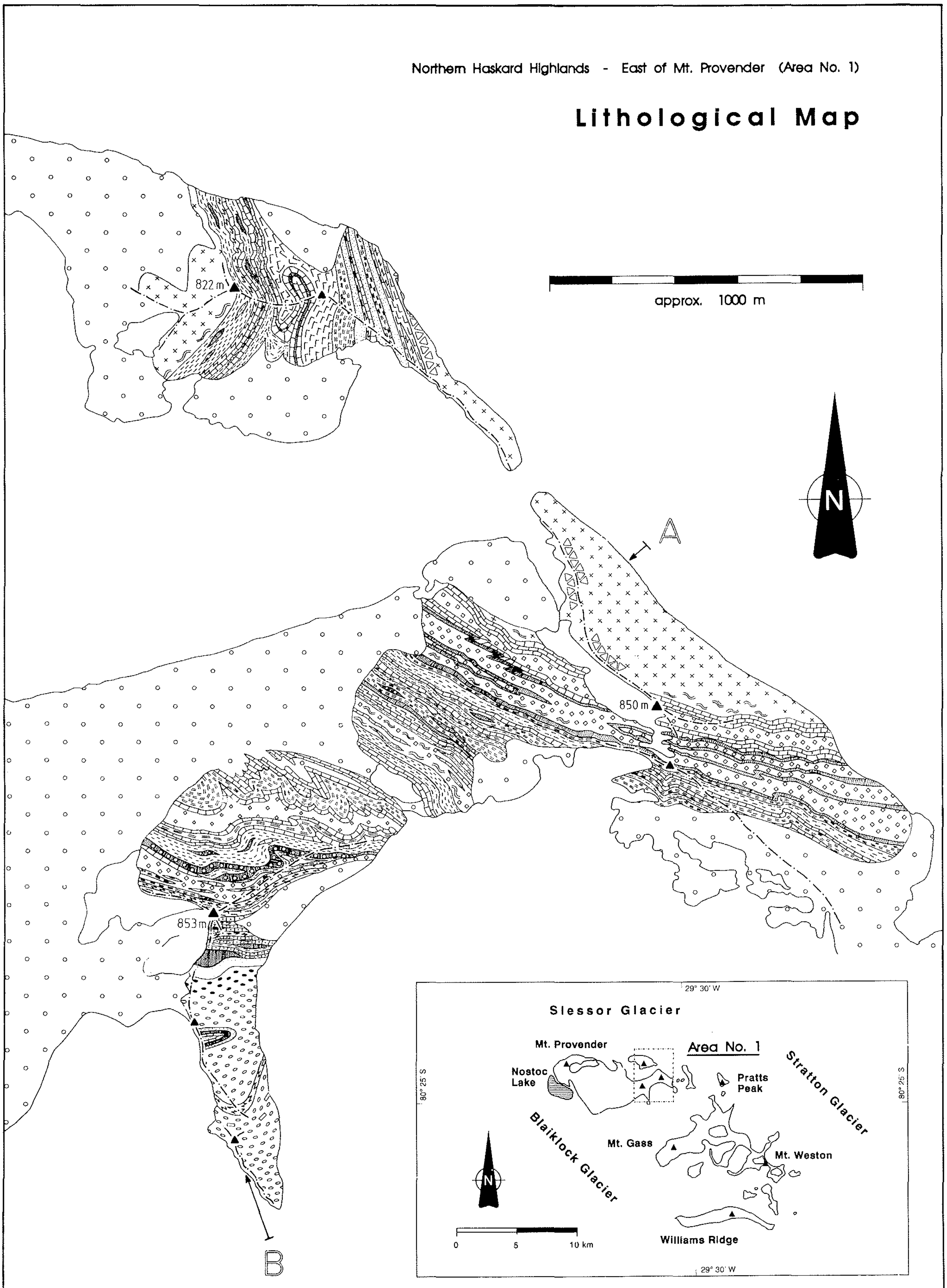

Fig. 26: Lithological map of Area 1, Haskard Highlands, northern Shackleton Range (geographical reference in Figs. 1 and 25); for legend see Fig. 29.

Abb. 26: Lithologische Karte des Gebietes 1, Haskard Highlands, nördliche Shackleton Range (geographischer Rahmen: Abb. 1 und 25). Legende in Abb. 29.

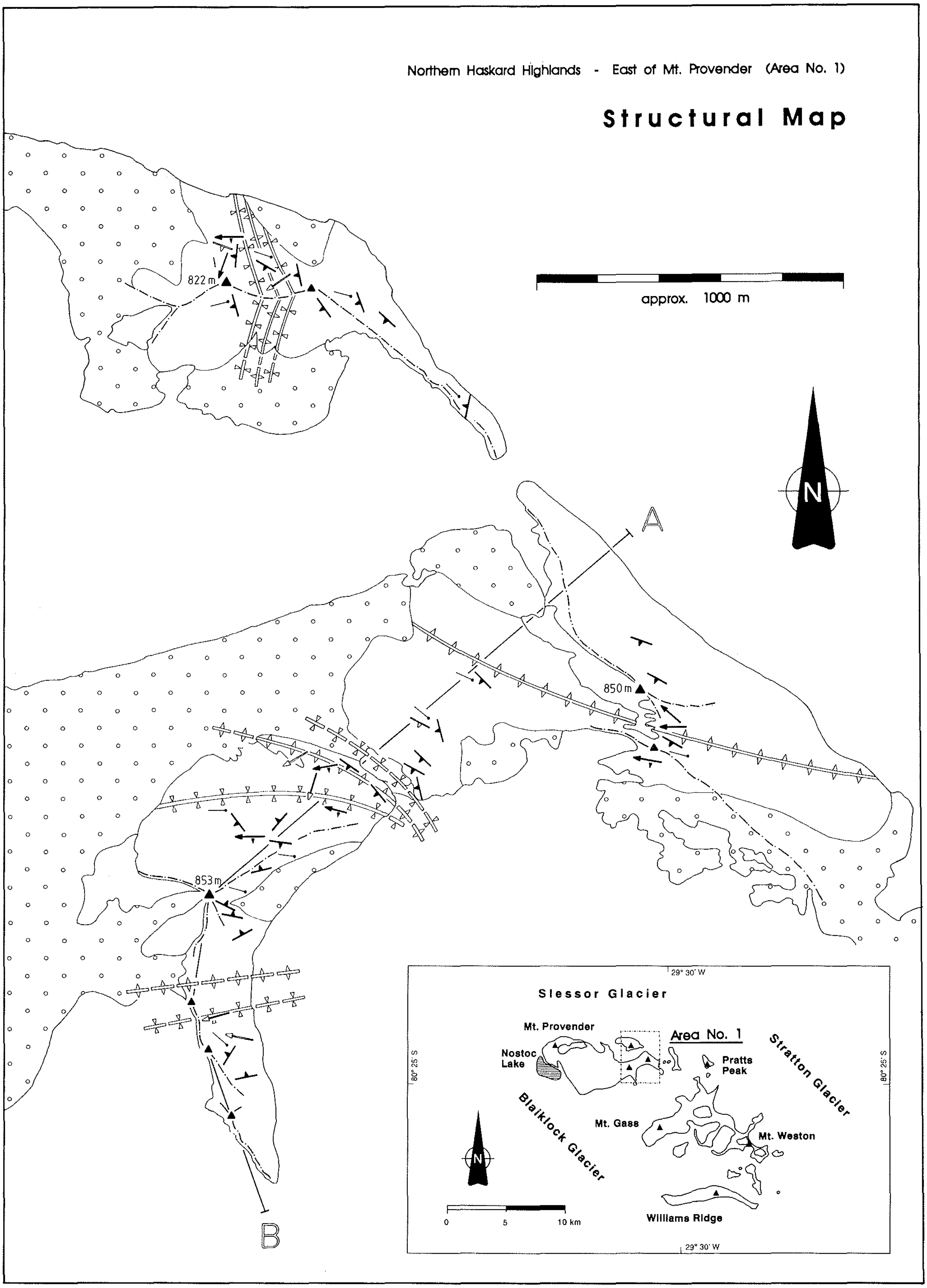

Fig. 27: Structural map of Area 1, Haskard Highlands, northern Shackleton Range (geographical reference in Figs. 1 and 25); for legend see Fig. 29.

Abb. 27: Strukturkarte des Gebietes 1, Haskard Highlands, nördliche Shackleton Range (geographischer Rahmen: Abb. 1 und 25). Legende in Abb. 29.

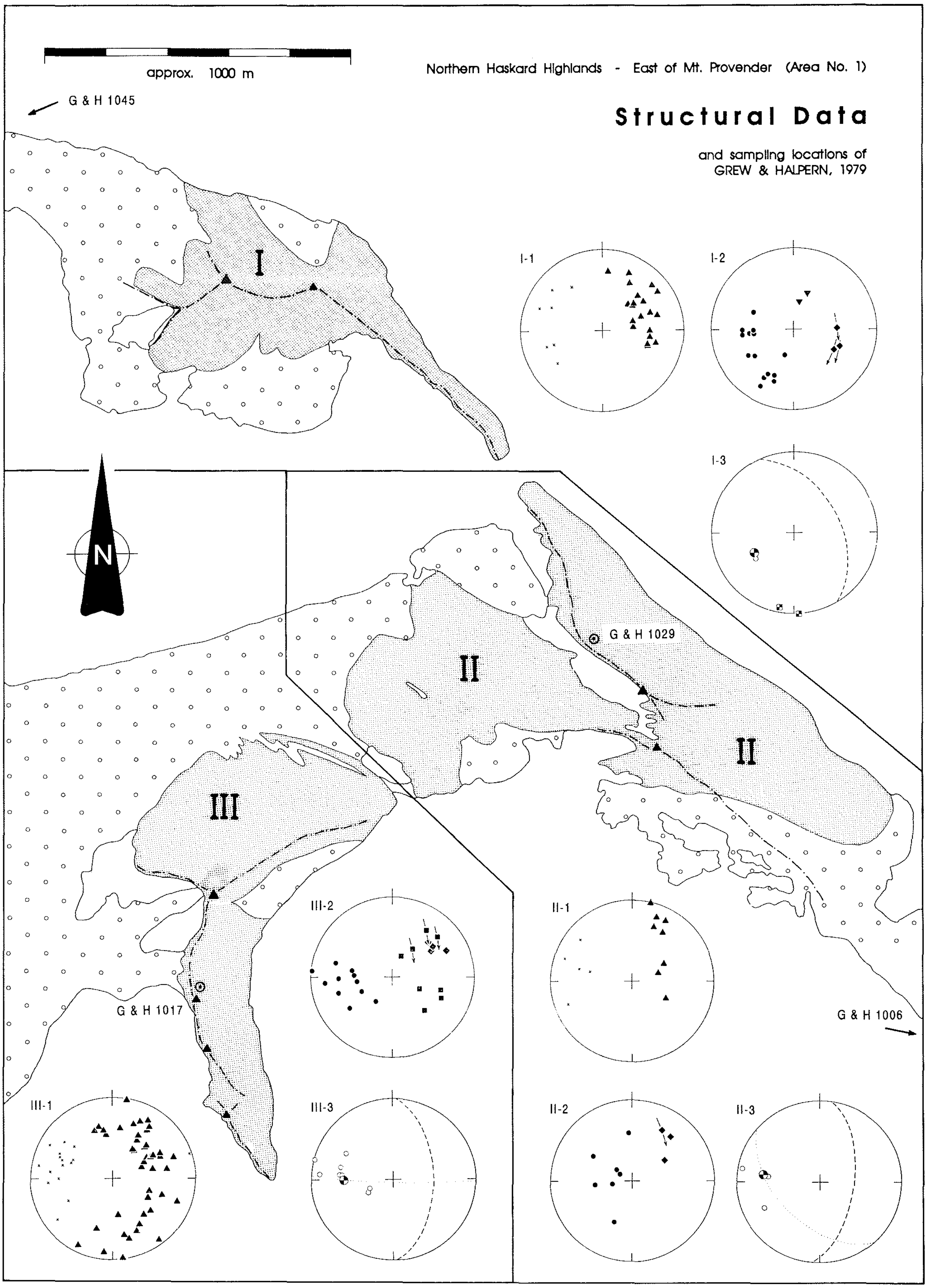

Fig. 28: Stereoplots (Schmidt net projections) for tectonic structures in Area 1, Haskard Highlands, northern Shackleton Range (geographical reference in Figs. 1 and 25), related to three phases of deformation (see text), for legend refer to Fig. 29.

Abb. 28: Gefügedaten aus Aufschlüssen in Gebiet 1, Haskard Highlands, nördliche Shackleton Range (geographischer Rahmen: Abb. 1 und 25). Darstellung im Schmidt'schen Netz, unterschieden nach drei Deformationsphasen. Legende in Abb. 29.

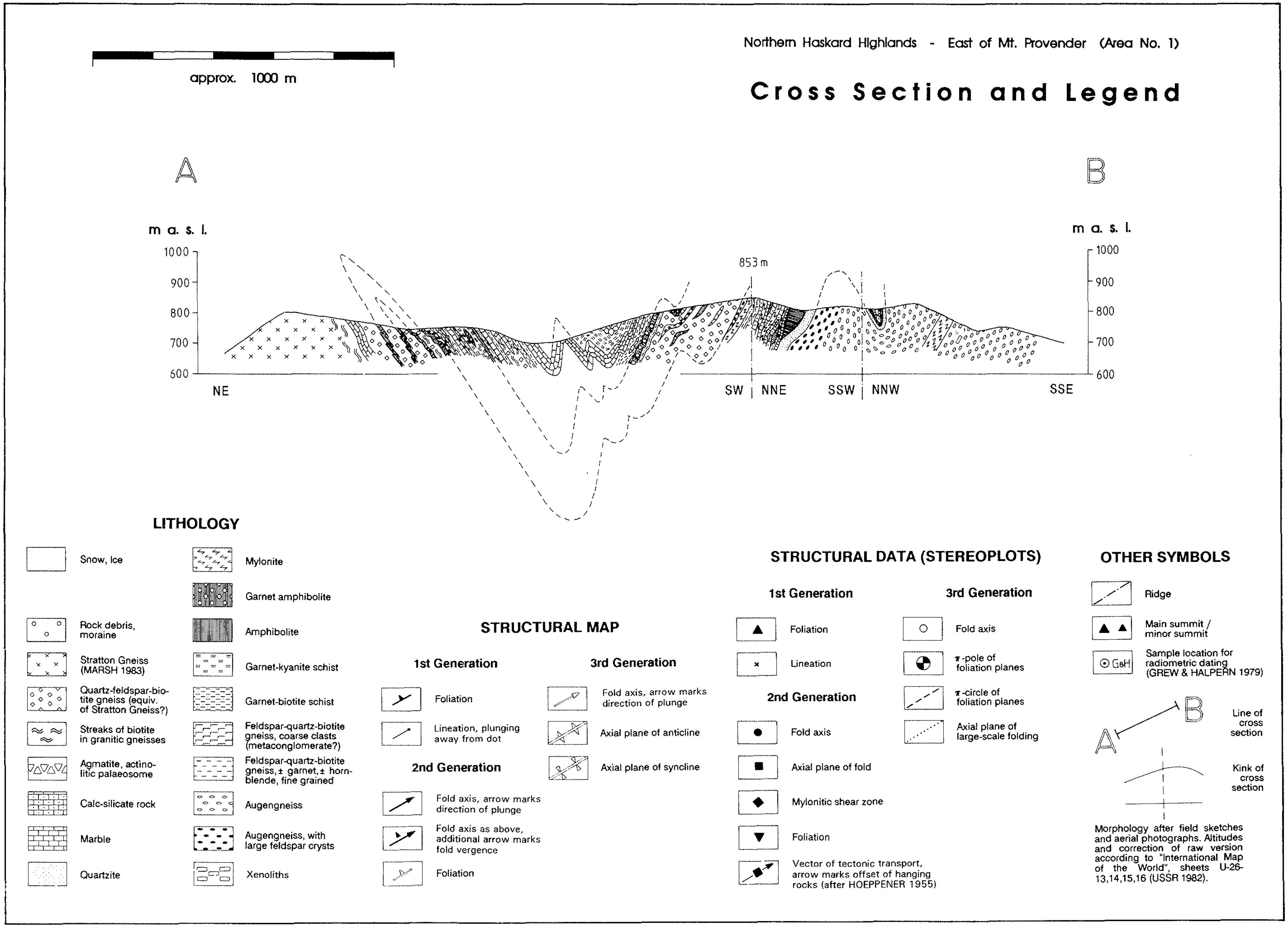

Fig. 29: Cross section through outcrops in Area 1, Haskard Highlands, northern Shackleton Range (geographical reference in Figs. 1 and 25). The section line is shown in Fig. 27. This figure also contains the legend for Figs. 26 through 28.

Abb. 29: Geologisches Profil durch das Gebiet 1, Haskard Highlands, nördliche Shackleton Range (geographischer Rahmen: Abb. 1 und 25). Lage der Profillinie s. Abb. 27; die vorliegende Abbildung enthält auch die Legende für Abb. 26 bis 28.

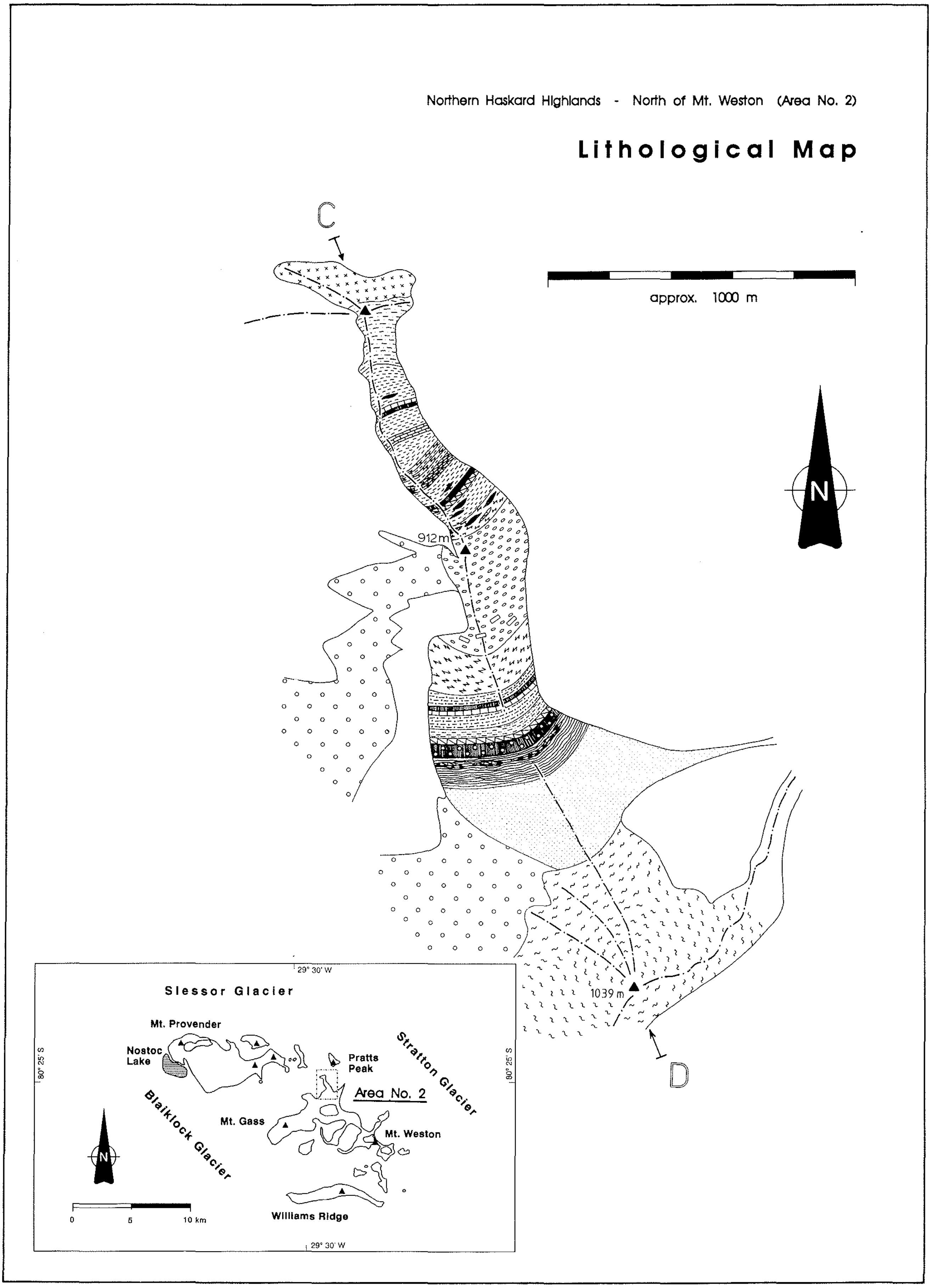

Fig. 30: Lithological map of Area 2, Haskard Highlands, northern Shackleton Range (geographical reference in Figs. 1 and 25); for legend see Fig. 33.

Abb. 30: Lithologische Karte des Gebietes 2, Haskard Highlands, nördliche Shackleton Range (geographischer Rahmen: Abb. 1 und 25). Legende in Abb. 33.

height 1039 consists of muscovite schists intercalated with lenses of biotite schists, amphibolites, marbles, and quartzose rocks. Due to an appreciable cover of debris, it is not clear whether there is a sharp boundary between the quartzite and muscovite schists or whether the composition changes gradually.

A garnet amphibolite layer crops out several metres S of the saddle between heights 912 and 1039. Garnets measure 2-3 mm in diameter and show no sign of deformation. The saddle is marked by slaty carbonate schists. They contain rounded blocks of roughly the same lithological composition, some of which are more resistant and rise about 1 m above the surrounding ground level (Fig. 31). This particular morphology is believed to be caused by exfoliation (cf. MIOTKE 1988: Fig. 5). The extremely fine-grained carbonate matrix contains elongated, disrupted, and folded rock relics (quartzose ribbons and dark pelitic schists). After reconstruction of the original orientation of the sediments, the sense of tectonic transport is northwestward.

The lower half of the southern flank of height 912 displays schists with variable amounts of garnet. In contrast to the rocks further S, the percentage of white mica is minimal. Garnets reach 1 cm average diameter and have asymmetric pressure shadows. Quartz lenses are rotated and form δ clasts (PASSCHIER & SIMPSON 1986). The summit area of height 912 consists of a compact gneiss with a reddish, fine-grained matrix, containing large feldspars, scattered garnet and hornblende crystals. Flattened xenoliths and the general macroscopic aspect suggest that this gneiss is identical to the augen gneiss described from Area 1 (section 3.2.1.1). A broad mylonitic zone marks the southern contact between augen gneiss and metasediments. It is accompanied by some discrete shear zones within the gneissic body itself.

A series of biotite(-garnet) schists and gneisses, mylonites, and layers of marble and amphibolite crops out north of height 912. The carbonates are usually medium to coarsely crystallized, but mylonitic and slightly schistose varieties prevail close to the summit. The foliation within amphibolites mainly results from oriented growth of prismatic actinolite. Often it is attenuated by bright feldspar ribbons. Black rock pods about 5-10 m across consist of coarsely crystallized pyroxene and amphibole. They are possibly genetically related to the pyroxenite body at Pratts Peak (MARSH 1983a).

At the northern end of the ridge, medium- and fine-grained gneisses with pinhead-sized garnets show a streaky biotite foliation. Since these gneisses are lithologically similar to the Stratton Gneiss, the contact with the metasediments is assumed to be of magmatic origin.

Fig. 31: Calcareous mylonite in the saddle between heights 912 and 1039 N of Mount Weston, Haskard Highlands, northern Shackleton Range; a = massive blocks of calcareous mylonite protrude from a schistose matrix of generally the same material. The mylonitic zone is about 5 m wide (length of hammer in foreground is 60 cm). Westward view along strike. b = detail of calcareous mylonite; the fine-grained calcitic matrix contains disrupted and folded pieces of schistose rock, as well as rotated and asymmetrically elongated quartz aggregates; pen parallel to subvertical foliation; length of pen is about 15 cm.

Abb. 31: Kalkmylonit im Sattel zwischen den Höhen 912 und 1039 nördlich Mount Weston, Haskard Highlands, nördliche Shackleton Range: (a) massige Kalkmylonit-Blöcke, umgeben von einer schiefrigen Matrix ungefähr gleicher Zusammensetzung. Breite der mylonitisierten Zone ca. 5 m (Länge des Hammers im Vordergrund 60 cm). Blick nach Westen parallel zum Streichen. (b) Detailaufnahme des Kalkmylonits. Die extrem feinkörnige Calcit-Matrix enthält zerrissene und verfaltete Gesteinsbruchstücke, und assymmetrisch gelängte Quarz-Aggregate. Stift liegt parallel zur Schieferungsrichtung, Länge 15 cm.

3.2.2.2 Structure

The foliation is roughly parallel to the lithological boundaries. The strike is NE-SW to E-W and the dip is steep N or S or vertical. Close to the summit of height 1039, the foliation dips locally westward at low angles. Lineations mostly trend E-W (Fig. 32, stereoplot I). σ clasts and asymmetrically elongated feldspars, as well as foliated phacoids („foliation fishes", HANMER 1986) can serve as shear sense indicators (SIMPSON & SCHMID 1983, PASSCHIER & SIMPSON 1986). Shear directions along the ridge vary between sinistral and dextral.

Fold axes reconstructed from the orientation of foliation planes

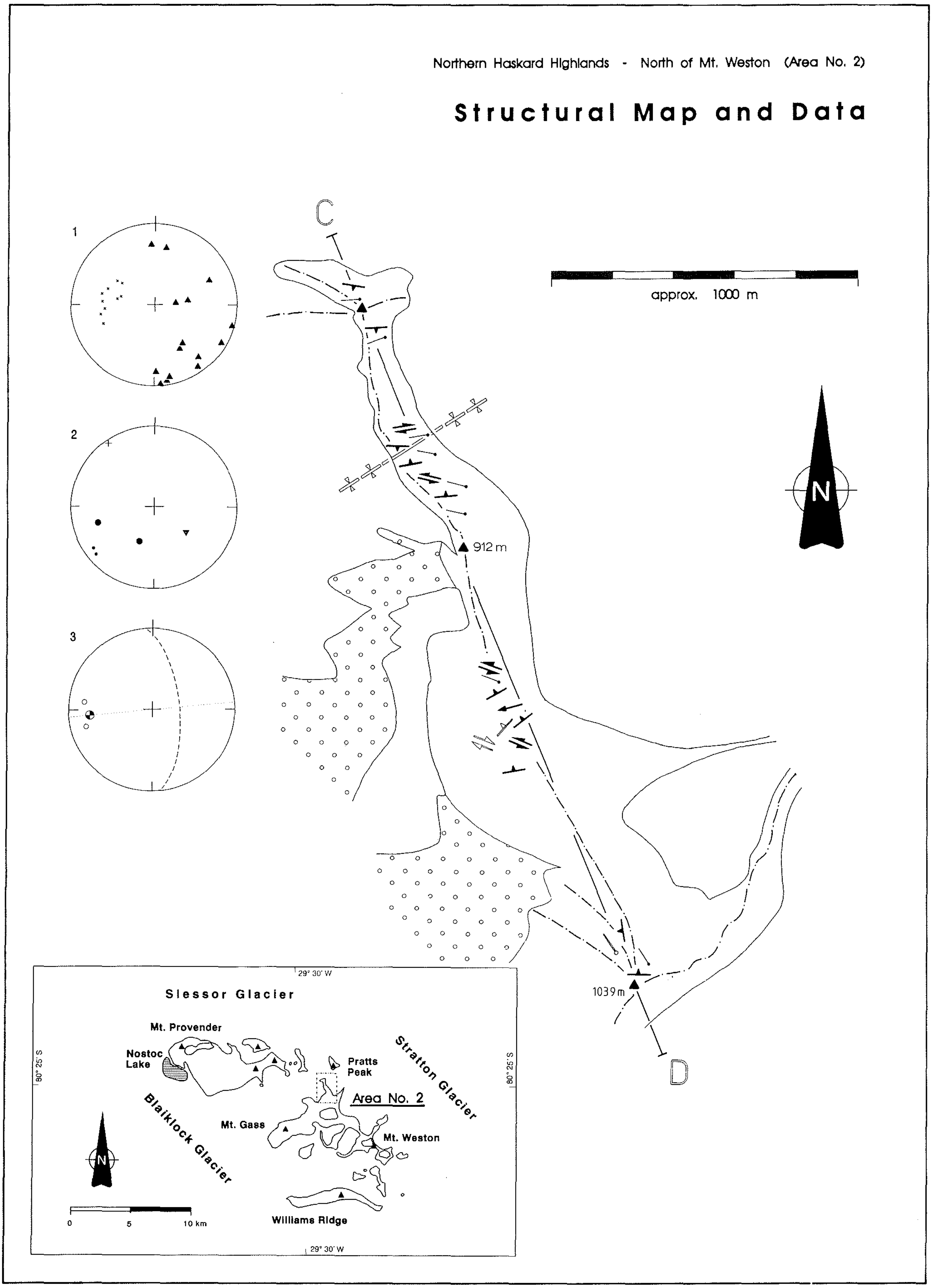

Fig. 32: Stereoplots (Schmidt net projections) for tectonic structures in Area 2, Haskard Highlands, northern Shackleton Range (geographical reference in Figs. 1 and 25), related to three phases of deformation (see text); for legend refer to Fig. 33.

Abb. 32: Strukturkarte und Gefügedaten des Gebietes 2, Haskard Highlands, nördliche Shackleton Range (geographischer Rahmen: Abb. 1 und 25). Darstellung im Schmidt'schen Netz, unterschieden nach drei Deformationsphasen. Legende in Abb. 33.

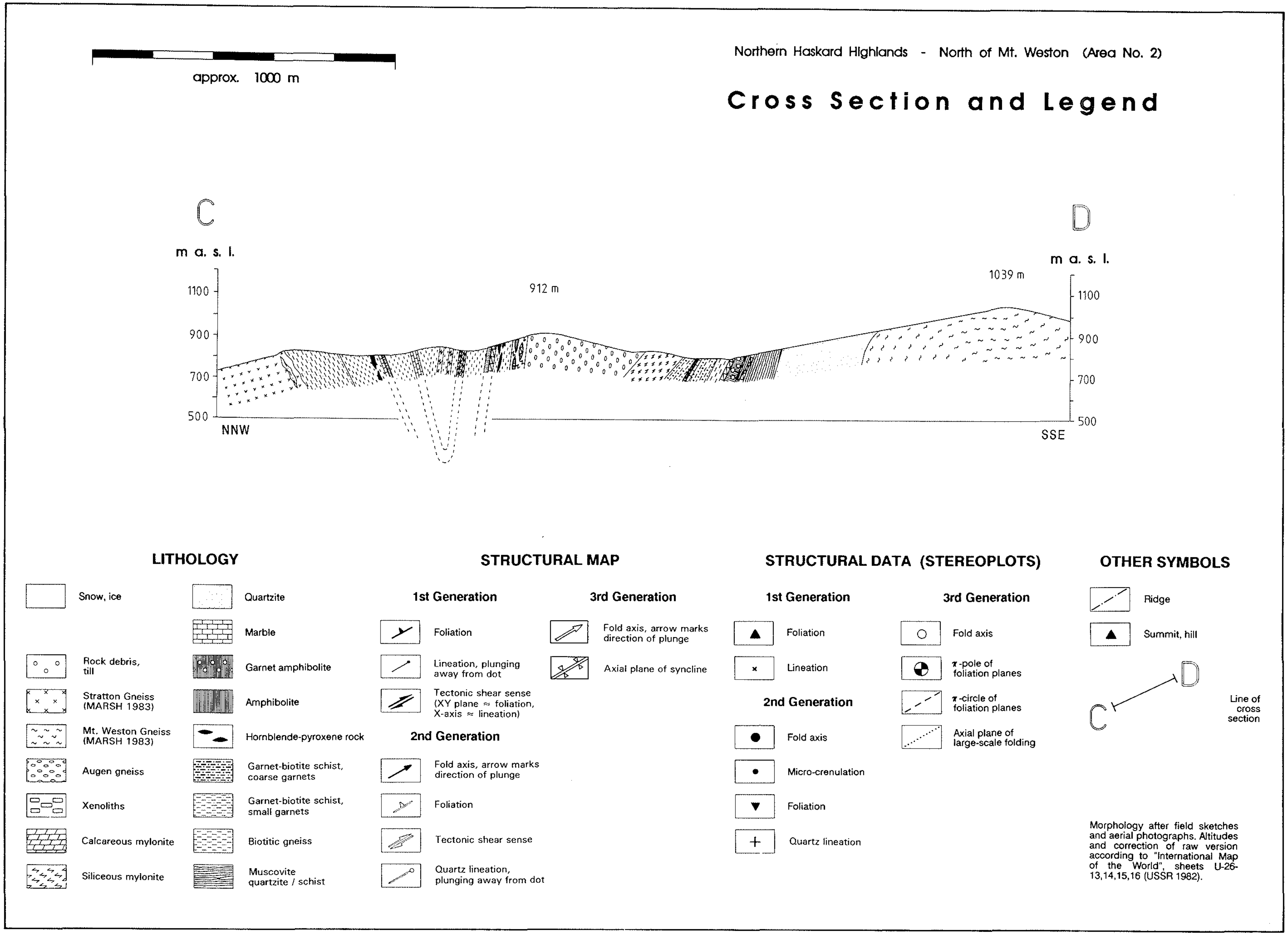

Fig. 33: Cross section through N-S ridge in Area 2, Haskard Highlands, northern Shackleton Range (geographical reference in Figs. 1 and 25). The section line is shown in Fig. 32. This figure also contains the legend for Figs. 30 and 32.

Abb. 33: Geologisches Profil durch Gebiet 2, Haskard Highlands, nördliche Shackleton Range (geographischer Rahmen: Abb. 1 und 25). Profillinie s. Abb. 32; die vorliegende Abbildung enthält auch die Legende für Abb. 30 und 32.

(i.e. π-poles) plunge gently W (stereoplot 3 in Fig. 32). Minor folds with this orientation have not been observed in the field, but from the general cross section (Fig. 33) it is clear that N of height 912 there is a large synclinal fold. Its axial plane is subvertical, and the amplitude is in the range of hundreds of metres (cf. Area 1). The southern limb contains several shear zones parallel to the foliation. The gentle fold within the Mount Weston Gneiss is homoaxial with the tight and upright fold further N. The discovery of large-scale folding explains the apparent inconsistency of shear sense indicators along the ridge (see above): if rotated into their original position, ductile fabrics point to overriding tectonic transport parallel to the lineation, i.e. from SE to NW.

A rectangular Z-shaped fold with short limbs about 5 m long between heights 1039 and 912 has axes plunging 30-45° SW. Since these axes plot SW of the lineation (stereoplot 2 in Fig. 32), and folding has SE vergency, this fold is assumed to represent an intermediate stage of deformation (cf. Area 1). Rocks near the double fold show a widely spaced, second foliation dipping NW.

3.2.3 Area between Mount Weston and Mount Gass (Area 3)

3.2.3.1 Lithology

According to the map of Marsh (1983a) and investigations by the present author, rocks belonging to the Mount Weston Gneiss crop out in the eastern part of height 888 (cf. Area 2). Mount Weston Gneiss gradually changes towards NW into schists and gneisses. Quartzites, quartz-rich gneisses, mica schists, and amphibolites are interleaved W of the summit of height 888. The thicknesses of the individual layers range from several cm to several m. As in the area N of Mount Weston, schistosity planes are coated with muscovite. Pure quartzites and garnet amphibolites occur west of the prominent carbonate layer that crops out on the N flank of height 888. The N-S ridge on which height 847 occurs roughly follows the axial plane of the so-called Mount Gass Fold (Marsh 1983a), and therefore an inverse succession of rocks is to be expected further to the W.

3.2.3.2 Structure

Several small cliffs on the north side of height 888 (Fig. 34) provide ideal exposures for studying the interaction between macroscopic deformation and metamorphism.

The degree of ductile shear deformation increases towards the W from the summit of height 888. Large phacoid-like boudins (type II A, Hanmer 1986) formed simultaneously with slightly smaller, amphibolitic boudins (Fig. 35). The assymmetric shapes indicate NW (downward) transport of the overlying rocks. Boudin „axes" (identical with the Y-direction of the overall deformation) are perpendicular to the lineation, which is marked by varying amounts of muscovite on foliation planes.

In other places amphibolite layers remain intact. Tectonic stress was concentrated on the gneissic areas in between, which reacted by isoclinal folding with axes parallel to the lineation („F1" in this outcrop). Later, amphibolite layers were fractured at right angles to the main foliation. These cracks penetrate the neighbouring gneisses and crosscut the isoclinal „F1" folds (Fig. 36).

The whole stack of metamorphic rocks has been folded twice. As in Areas 1 and 2, „F2" fold axes plot somewhat further SW than the lineations. Under ideal circumstances, the small intersection angle can be directly observed in outcrops (Fig. 37). The amplitudes of late „F3" folds vary between 0.5 and 50 m. Examples of this generation can be seen on the maps in Fig. 34 and 38, and also the large Mount Gass Fold *sensu* Marsh (1983a) belongs to this generation.

3.3 *Tectonostratigraphic units in the northern Haskard Highlands*

3.3.1 Introductory remarks

Marsh (1983a) established a framework of protostratigraphic units that is based mainly on lithology. Since tectonic processes played a major role in the history of the northern Shackleton Range, it was of interest to check whether Marsh's approach also reflects the tectonostratigraphic structure of the region. The ridge between Mount Weston and Pratts Peak (Area 2) is particularly suitable for this. The Mount Weston Gneiss, Mount Gass Formation, and Nostoc Lake Formation (in the sense of Marsh 1983a) appear to form a continuous succession from bottom to top. It is convenient to divide into five sub-areas:

- Sub-Area A: the upper part of height 1039 (Mount Weston Gneiss);
- Sub-Area B: the lower part of the northern slope of height 1039 (Mount Gass Formation);
- Sub-Area C: the carbonate mylonite in the saddle between heights 1039 and 912 (Mount Gass Formation);
- Sub-Area D: the lower part of the southern slope of height 912, including the wide zone of mylonitic schists (Mount Gass Formation);
- Sub-Area E: the summit area of height 912 and the ridge further north (Nostoc Lake Formation).

Each of these sub-areas represents a more or less homogeneous succession of rocks uninterrupted by tectonic boundaries.

3.3.2 Characteristic microfabrics

Sub-Area A

The macroscopic planar fabric of the Mount Weston Gneiss is dominated by thin layers of felted, randomly oriented fibrolite needles (sillimanite$_2$) and possibly also very small muscovite (sericite) flakes. These layers, anastomosing between feldspar- and quartz-rich areas, are typically 0.5-1.0 mm thick and several mm up to a few cm apart. In some places, interstitial fibrolitic material occurs between feldspar and quartz grains.

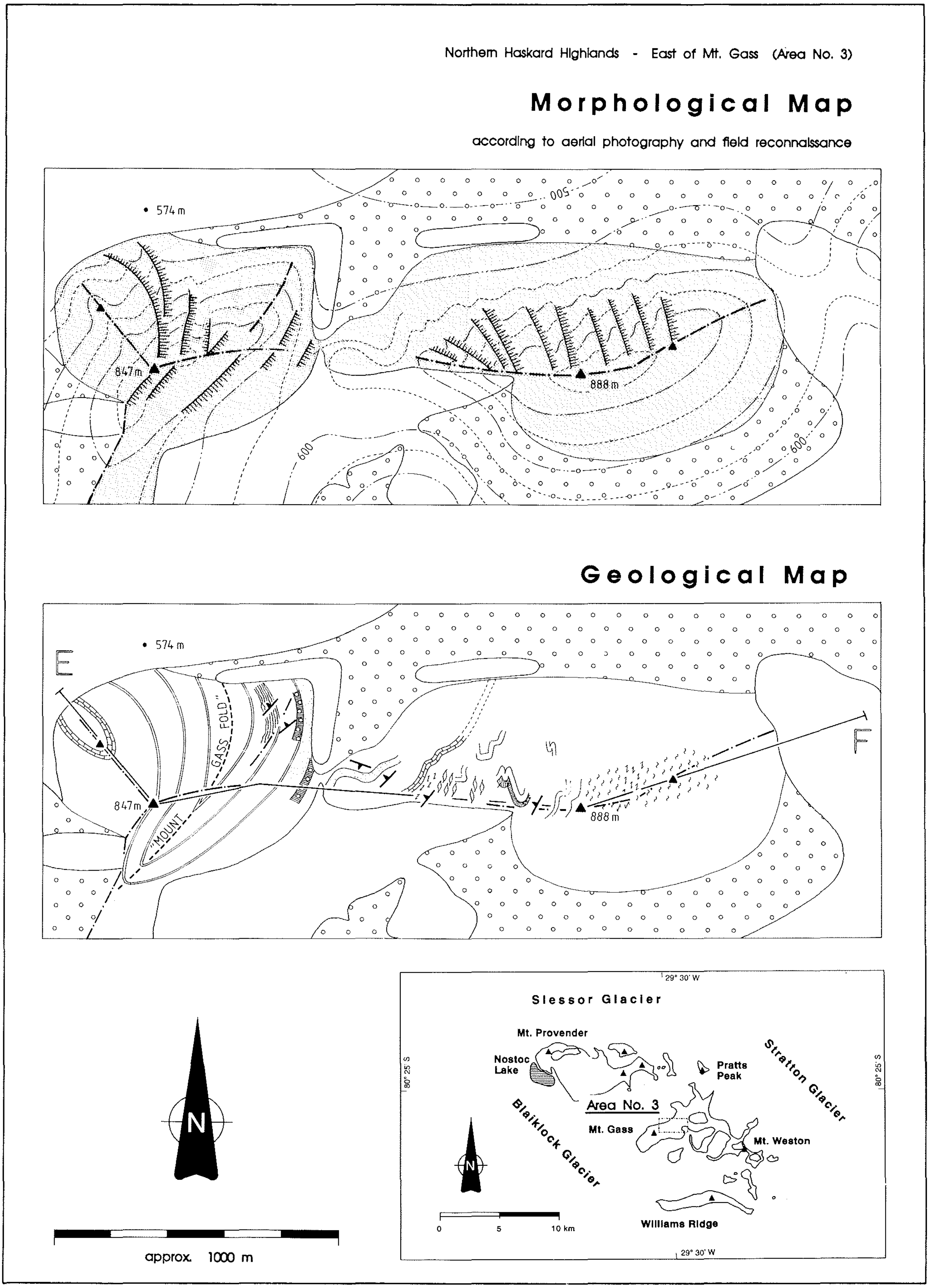

Fig. 34: Schematic morphological and geological maps of Area 3, Haskard Highlands, northern Shackleton Range (geographical reference in Figs. 1 and 25); for legend see Fig. 38.

Abb. 34: Schematisierte morphologische Karte und geologische Details des Gebietes 3, Haskard Highlands, nördliche Shackleton Range (geographischer Rahmen: Abb. 1 und 25). Legende in Abb. 38.

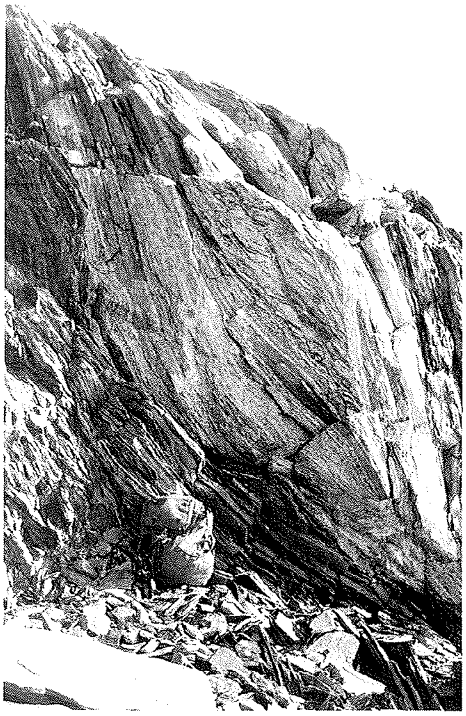

Fig. 35: Two styles of boudinage in the N face of height 888 between Mount Gass and Mount Weston, Haskard Highlands, northern Shackleton Range. Shape asymmetry indicates NNW transport of the overlying rocks (clockwise sense of shear in this view). a = large phacoid with preserved internal layering („foliation fish"). See rucksack for scale. b = boudinage of competent amphibolitic layer. Note bright zone of syn-tectonic feldspar crystallization between boudins. Length of pen is about 15 cm.

Abb. 35: Boudinage am Nordhang der Höhe 888 zwischen Mount Gass und Mount Weston, Haskard Highlands, nördliche Shackleton Range. Assymmetrie der Boudins belegt NNW-Transport des Hangenden (in dieser Ansicht = rotationale Deformation im Uhrzeigersinn). (a) Großer Phakoid-Körper mit internem Lagenbau („foliation fish"). Rucksack als Maßstab. (b) Boudinage einer kompetenten, amphibolitischen Lage, mit syntektonischer Feldspat-Kristallisation zwischen den einzelnen Boudins. Länge des Stiftes 15 cm.

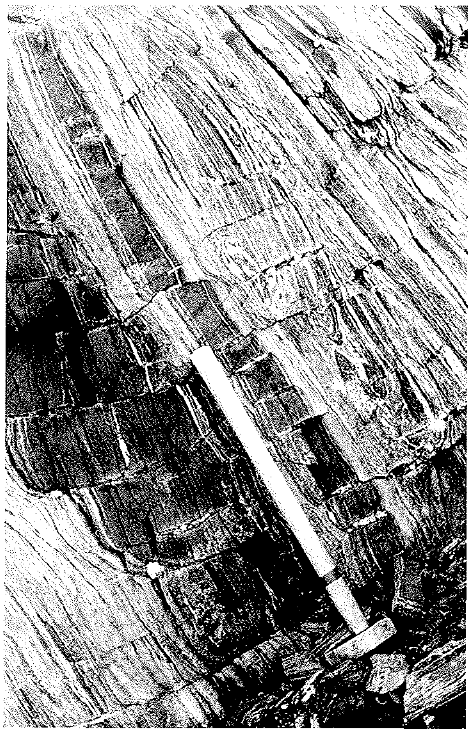

Fig. 36: NNW transport of the overlying rocks parallel to the compositional layering results in different styles of deformation, depending mainly on rheological differences: Incompetent gneissic layers react by internal ductile folding, while competent amphibolites show brittle shear fractures and „stack of books" rotation (clockwise in this view). N face of height 888 between Mount Gass and Mount Weston, Haskard Highlands, northern Shackleton Range. View towards W along slope.

Abb. 36: Lagen-paralleler, NNW-gerichteter duktiler Transport der überlagernden Gesteine erzeugt - in Abhängigkeit von den rheologischen Eigenschaften - unterschiedliche Deformationsgefüge. Inkompetente Gneis-Lagen werden intern verfaltet, während kompetente Amphibolit-Lagen spröde zerbrechen und „Buchstapel"-ähnlich rotieren (in dieser Ansicht im Uhrzeigersinn). Nordhang der Höhe 888 zwischen Mount Gass und Mount Weston, Haskard Highlands, nördliche Shackleton Range. Hang-paralleler Blick nach Westen.

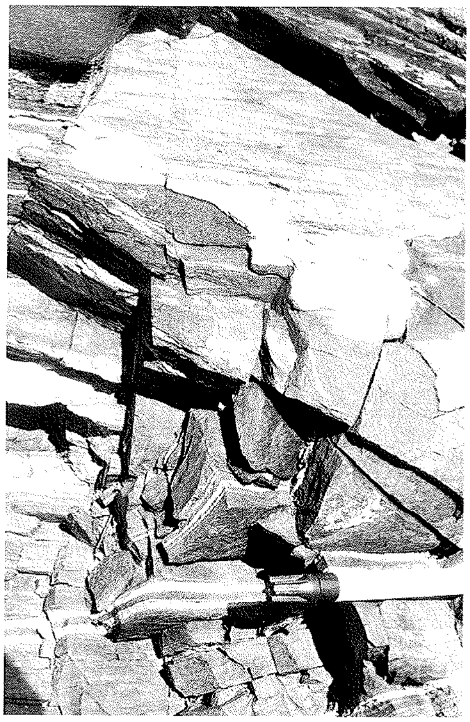

Fig. 37: Tight fold with SW-plunging fold axis (pen parallel to axis; SW = right side of picture). Muscovitic lineations on quartzose layers are not ideally parallel, but show a deviation of 10-20°. N face of height 888 between Mount Gass and Mount Weston, Haskard Highlands, northern Shackleton Range.

Abb. 37: Enge Falte mit nach SW abtauchender Achse (Stift parallel zur ‚Achse, SW = rechte Bildseite). Die linearen Muskovit-Streifen verlaufen nicht exakt parallel zu den Faltenachsen, sondern schließen mit diesen Winkel von ca.10-20° ein. Nordhang der Höhe 888 zwischen Mount Gass und Mount Weston, Haskard Highlands, nördliche Shackleton Range.

The following minerals are included within the fibrolitic bands and are obviously older than these: garnet$_1$, spinel, magnetite/ilmenite, prismatic sillimanite$_1$, and staurolite$_1$. Some garnets show cores rich in quartz and magnetite inclusions (garnet$_1$), and inclusion-free rim zones (garnet$_2$). The latter overgrow biotite$_1$ flakes that - in contrast to contemporaneous biotite$_2$ grains - are rich in magnetite inclusions. Garnet$_1$, brown-coloured spinel, and magnetite/ilmenite occur exclusively as fragments of large blasts embedded in fine-grained biotite$_{2?}$ coronas. The outlines of these biotite zones are sometimes irregular or, in other cases, determined by the shape of embedded mineral relics rather than influenced by deformation. In contrast to the former minerals, late staurolite$_2$ and prismatic sillimanite$_1$ are only slightly deformed and are not surrounded by biotite coronas. The relatively large size of staurolite$_2$ blasts points to static crystallization, probably correlatable with the generation of inclusion-free garnet$_2$ rims.

Some elongated feldspar blasts in the feldspar-quartz dominated country rock have asymmetric pressure shadows filled with equigranular quartz. Other feldspars are broken and show bookshelf rotation of the fragments. In both cases, NW tectonic transport of the overlying rock is indicated.

Sub-Area B

Old garnet grains form the cores of asymmetrically elongated zones, which are due to NW-vergent shear deformation. One fish-like lens shows an internal planar fabric with an angle of about 45° with the foliation outside (Fig. 39). Some competent metamorphic layers are sheared off along small-scale ecc planes (Platt 1984).

Sub-Area C

Owing to intense dynamic recrystallization, the tectonometamorphic evolution of this unit previous to NW-directed ductile shearing is unclear. Similar to the rocks further S, and in contrast to all rock types further N, the carbonate mylonites contain an unusually high proportion of magnetite fragments. The extremely minute size of recrystallized calcite grains suggests deformation persisted until late stages of metamorphism, but the migration of grain boundaries may also have been blocked to a certain extent by magnetite particles.

Sub-Area D

Hornblende, monomineralic quartz lenses, feldspar, and garnet$_1$ - the latter two as unbroken crystals or as brittle fragments - serve as rigid centres of SE-vergent σ-clasts created during the dominating tectonometamorphic event. Syntectonic garnet$_2$ rotates under NW-vergent shear and forms typical δ-clasts. Solitary biotite$_1$ flakes oriented parallel to the planar fabric are present within older sillimanite grains. Kyanite forms single prisms, as well as hypidioblastic rims around pre-existing sillimanite. Quartz aggregates show grain elongation and dynamic recrystallization. A few garnets contain angular orthopyroxene fragments of unknown significance (see below). Some feldspar-rich regions have a grain-orientation fabric that is oblique to the general layering and foliation.

The sense of late shearing is SE, i.e. opposite to that of the stage of pervasive ductile deformation. Garnets$_{1+2}$ and other rigid grains are cut by discrete shear fractures, whereas the rock in general is crossed by ductile shear bands with high magnetite contents and by new biotite$_2$ and iron-rich chlorite grains. Post-tectonic crystallization leads to the formation of inclusion-free garnet$_3$ rims, and poikiloblastic quartz grains overgrow garnets$_{1+2}$, kyanite, and feldspar. Feldspar and quartz grains with lattice deformation recrystallize under static conditions.

Sub-Area E

The original, partially idiomorphic grain shapes and the initial (growth) orientations of the main minerals within this sub-area are preserved except where retrograde reactions or annealing have taken place. Plagioclase crystals show narrow twin lamellae. NW-vergent, foliation-parallel shear is responsible for kinking, fragmentation, and bookshelf rotation of feldspar crystals. Asymmetric pressure shadows are filled with quartz in pelitic schists and leucocratic gneisses and with feldspar in mafic rocks (amphibolites). Non-zoned garnet grains are crossed by quartz and feldspar bands parallel to the foliation. New biotite flakes, and narrow zones of intense feldspar recrystallization crosscut the dominant layering and foliation. Since these fabrics look similar to the late shear fabrics in Sub-Area D, they are also inferred to indicate southeastward tectonic transport.

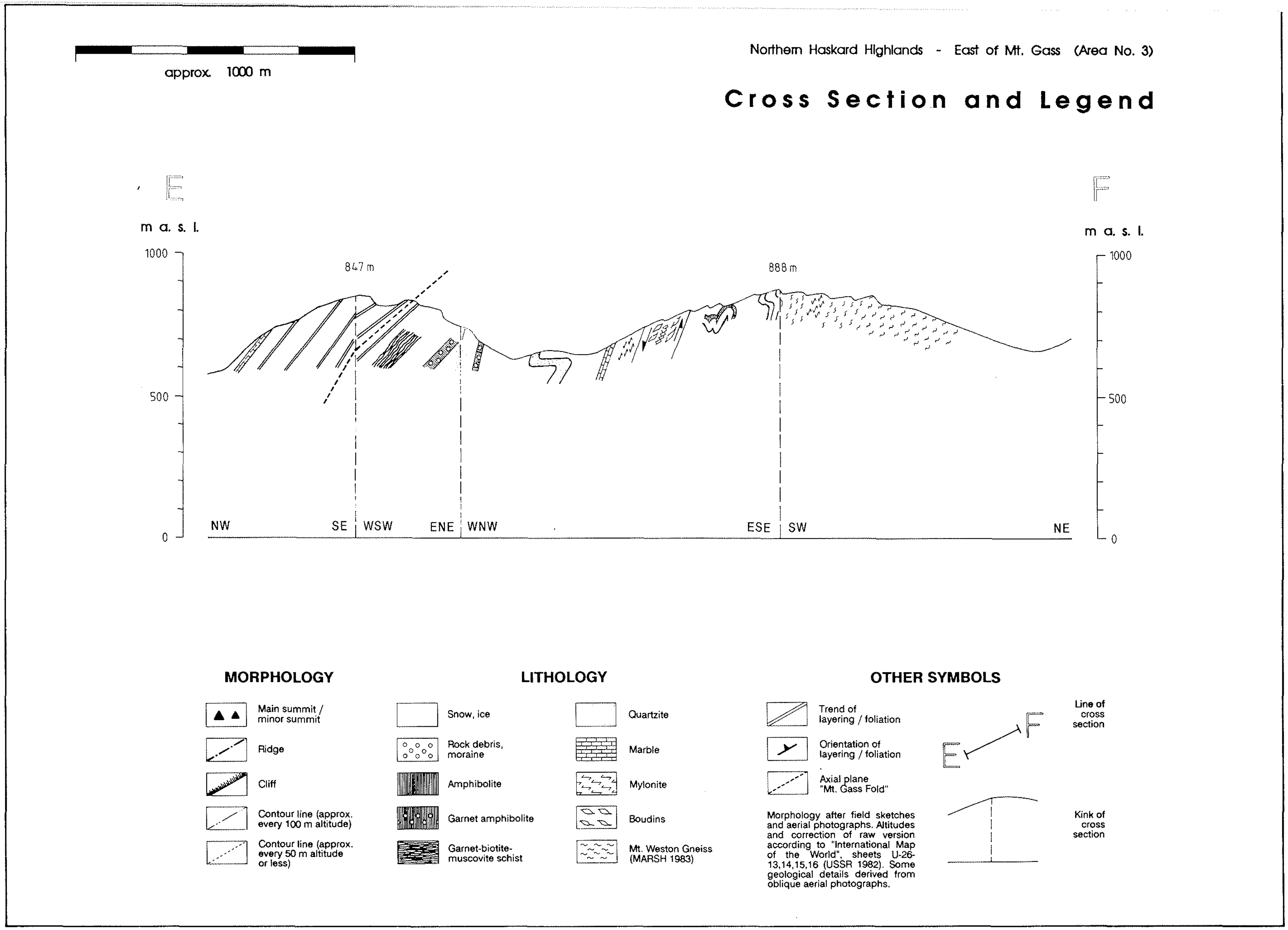

Fig. 38: Schematic cross section through E-W ridge in Area 3, Haskard Highlands, northern Shackleton Range (geographical reference in Figs. 1 and 25). The section line is shown in Fig. 34. This figure also contains the legend for Fig. 34.

Abb. 38: Schematisierter Schnitt durch das Gebiet 3, Haskard Highlands, nördliche Shackleton Range (geographischer Rahmen: Abb. 1 und 25). Lage der Profillinie s. Abb. 34; die vorliegende Abbildung enthält auch die Legende für Abb. 34.

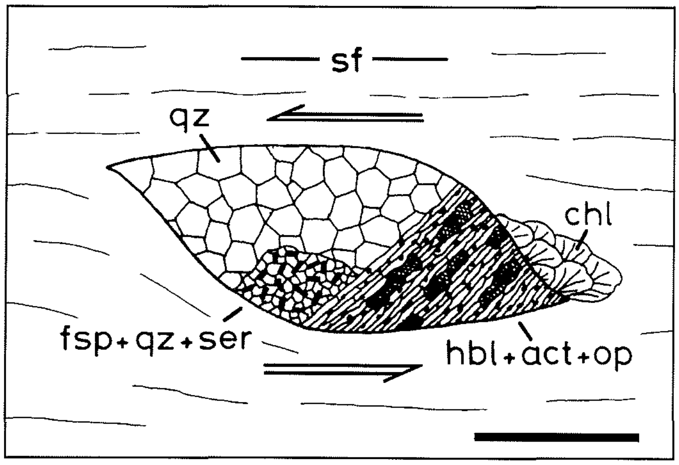

Fig. 39: Small detrital grain in biotitic schist from N of Mount Weston (Haskard Highlands, northern Shackleton Range); internal fabric made up of recrystallized quartz (qz), feldspar-quartz-sericite aggregate (fsp+qz+ser), and a zone of oriented hornblende and actinolite, including some opaques (hbl+act+op). Late-tectonic chlorite (chl) accentuates σ-shape formed during ductile NW thrusting (foliation = sf). Scale bar= 1 mm.

Abb. 39: Detritisches Korn in Biotitschiefern nördlich Mount Weston (Haskard Highlands, nördliche Shackleton Range). Quarz-Rekristallisat (qz), Feldspat-Quarz-Serizit-Aggregate (fsp+qz+ser), und orientierte Hornblende-/Aktinolith-Kristalle mit Opak-Einschlüssen (hbl+act+op) definieren ein vom umgebenden Gestein unabhängiges Interngefüge (sf = allgemeine Schieferung). Spät-tektonisch gewachsener Chlorit (chl) verstärkt die durch NW-gerichtete Scherung entstandene σ-Form.

Well-preserved orthoclase crystals with a single, median twin plane, as well as intergrowth of large plagioclase and garnet blasts, suggest that the rocks at the northern end of the ridge represent a granitoid intrusion (see cross-section in Fig. 33). Adjacent metamorphics show intense blastesis of secondary quartz and microcline blasts that overgrow pre-existing garnet, hornblende, and clinopyroxene, and are probably due to static heating (and fluid input?). Since microfabrics indicate that the igneous rocks were subjected to minor deformation, they must have been intruded during a late phase of the main tectonometamorphic event.

3.3.3 Tectonostratigraphic unit boundaries

On the basis of the observations discussed above, it is now possible to define probable tectonostratigraphic unit boundaries, as illustrated in a synoptic scheme similar to biostratigraphic tables (Fig. 40). It must be stressed that within this scheme, time information is related to each sub-area separately and does not refer to an overall schedule of events. It should also be noted that none of the features described can be used as a stand-alone criterion. Some rocks may, for example, be void of old mineral relics, since there was no earlier tectonometamorphism, but old fabrics may also be destroyed during a later event. The following major differences between Sub-Areas A-E were recognized (see also Fig. 40):

- Minerals that are potentially the product of an early metamorphic event (spinel, staurolite, orthopyroxene, magnetite/ilmenite) have been found in Sub-Areas A-D. Relict planar fabrics, however, are preserved only in Sub-Areas B and C.
- Muscovite flakes and high contents of magnetite are restricted to Sub-Areas A-C.
- Judging from the occurrence of magnetite, Sub-Areas B and C probably represent a continuous sedimentary series.
- Kyanite formed in rocks of appropriate bulk composition only in Sub-Areas D and E. It formed from sillimanite in Sub-Area D. Fibrolitic sillimanite occurs only in Sub-Area A.
- Most of the fabrics produced during NW-vergent shear are in Sub-Areas D and E (with less intense deformation in the latter).
- Late-metamorphic zones displaying SE-directed shear deformation are restricted to Sub-Areas D and E.
- Annealing of deformed quartz and feldspar occurs only in Sub-Areas D and E. Late static crystallization of relatively large mineral blasts is restricted to the same region.

In summary, the unit boundaries as deduced from the lithological composition by MARSH (1983a see Fig. 40, top rows) are widely supported by microstructure observations. Since there are definite differences between Sub-Areas B+C+D and Sub-Area E, speculation about a continuous sedimentary transition from the Mount Gass Formation to the Nostoc Lake Formation is not supported. An additional boundary seems possible between Sub-Areas B and D. In the case Sub-Areas B and C belong to the same unit, as suggested above, the unit boundary in fact lies between Sub-Areas C and D. Consequently, the Mount Gass Formation *sensu* MARSH (1983 a) can no longer be considered as a single unit, but has to be divided into two independent rock series with different structural histories.

3.4 *Radiometric dating*

Radiometric dating of rocks from the northern Haskard Highlands has yielded equivocal ages (GREW & HALPERN 1979, GREW & MANTON 1980, PANKHURST et al. 1983). This is partially due to the fact that the influence of later events on whole rock ages is hard to assess. Since many descriptions of sample locations and rock types are unfortunately superficial, it is difficult to correlate radiometric ages with observed fabrics and metamorphic minerals.

Rb-Sr whole-rock determinations on samples of Mount Weston Gneiss indicate an age older than 1550 Ma (PANKHURST et al. 1983), which is in accordance with Sm-Nd dates of about 1500 Ma from the same region (BELYATSKY pers. comm.). Rb-Sr ages for the Mount Gass Formation range from 900-1500 Ma (PANKHURST et al. 1983). There are three possible explanations for this relatively large time span:
(i) isotopic exchange between relics of an old metamorphic event and minerals grown during a later event,
(ii) isotopic exchange between clastic sedimentary minerals eroded from an old basement and younger metamorphic minerals, and

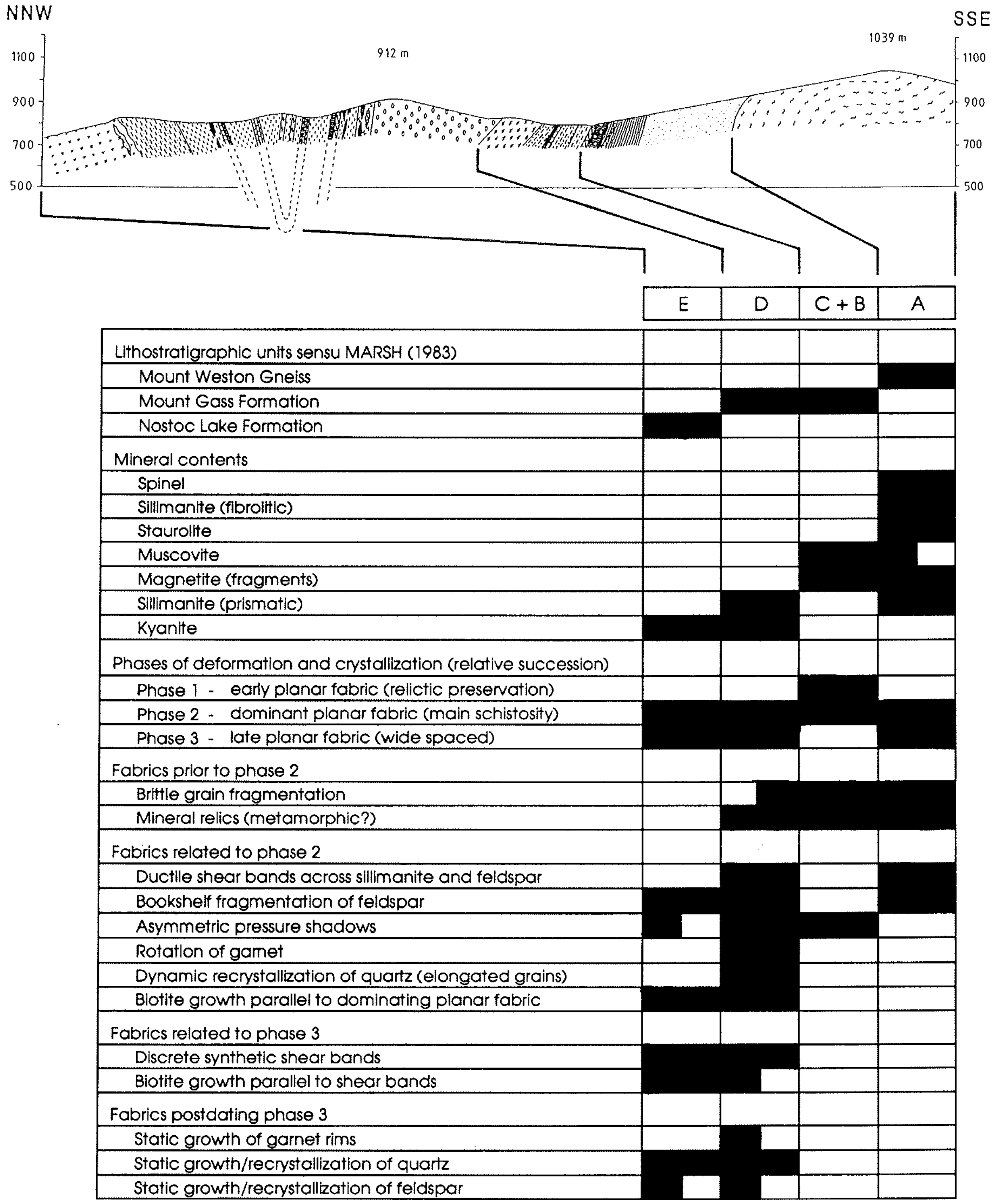

Fig. 40: Schematic synopsis of minerals and fabrics occurring in subareas A-E north of Mount Weston, Haskard Highlands, northern Shackleton Range; phases of deformation and crystallization were not integrated into an overall (absolute) time framework, but define the internal order of events in each region. For detailed geological information, refer to Fig. 33.

Abb. 40: Schematische Zusammenstellung von Mineralen und Gefügen innerhalb der Teilgebiete A bis E nördlich Mount Weston, Haskard Highlands, nördliche Shackleton Range (Gebiet 2). Die Einteilung in Deformations- und Kristallisationsphasen gilt jeweils nur innerhalb des betrachteten Teilgebiets, und bezieht sich nicht auf einen übergeordneten Zeitrahmen. Weitere geologische Informationen s. Abb. 33.

(iii) partial resetting of the isotopic clock during the late-metamorphic, non-pervasive shearing event.

At present, most of the radiometric ages have been obtained from rocks of the Nostoc Lake Formation; they range from about 655 Ma to about 430 Ma. However, only a few age determinations are available on isolated minerals which would allow a temperature-time curve to be determined. In order to obtain at least a rough idea of the possible time of tectonometamorphic events, the accumulated confidence levels of all published Rb-Sr determinations have been plotted (Fig. 41). Two major peaks at 528 Ma and 502 Ma are obtained. As a first, tentative interpretation, it is suggested that the early age represents the peak of amphibolite facies metamorphism and pervasive deformation, while the later age indicates partial reactivation by shear deformation and/or igneous intrusions (static grain growth). The sharp drop at about 490 Ma is caused by final closure of the Rb-Sr system. A „Beardmore" event, suspected by GREW & HALPERN (1979) and PANKHURST et al. (1983) on the basis of some ages of about 600 Ma, cannot be correlated with any structures observed in the field. Sm-Nd ages between 720 and 740 Ma (BELYATSKY pers. comm.) are also still in need of a satisfactory interpretation.

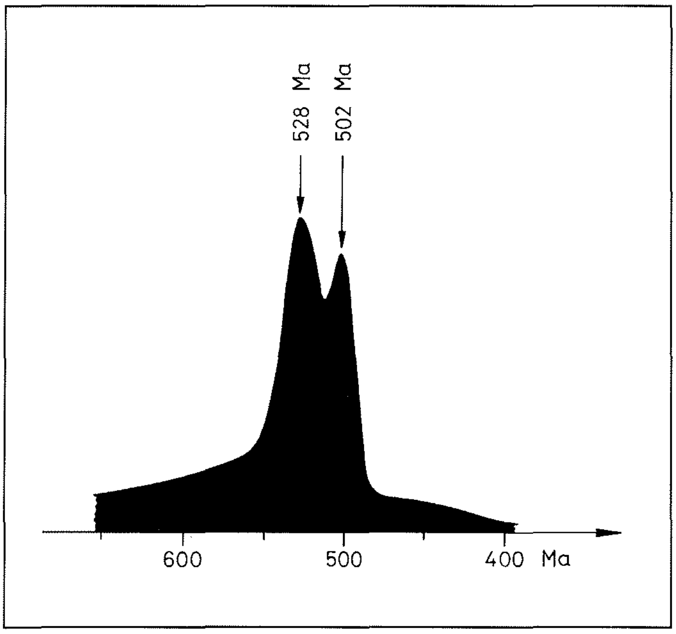

Fig. 41: Graph of Rb-Sr ages from the Nostoc Lake Formation, northern Shackleton Range, derived by superposing the standard distribution curves of all published measurements. Y-axis illustrates the „probability" of a significant event.

Abb. 41: Graphische Veranschaulichung der vorliegenden Rb-Sr-Datierungen aus der Nostoc Lake Formation, nördliche Shackleton Range. Die Kurve entstand durch Überlagerung der publizierten Einzeldaten (Normalverteilungs-Kurven unter Berücksichtigung der jeweiligen Fehlergrenzen). Die Auslenkung in Y-Richtung entspricht der „Wahrscheinlichkeit" eines Ereignisses zum gegebenen Zeitpunkt.

3.5 *Tectonometamorphic history of the northern Haskard Highlands - Discussion*

MARSH's (1983a) explanation of the tectonic history of the northern Haskard Highlands fit our results in so far as rocks in this area generally show fabrics of (at least) two generations. The microstructural observations and the radiometric ages clearly show that the Mount Weston Gneiss has an older tectonometamorphic history than the metasedimentary units further north. The Mount Weston Gneiss suffered high-grade metamorphism (coexisting sillimanite and K-feldspar) during the mid-Proterozoic. A second event of slightly lower metamorphic grade is documented in the fibrolitic separation planes and related fabrics.

The sedimentary units underwent amphibolite facies metamorphism during the Late Cambrian. Syn-metamorphic grain fabrics have been modified by pervasive NW-directed shear deformation, and by syn-tectonic mineral growth (e.g. garnet, biotite), especially in the Mount Gass Formation *sensu* MARSH (1983a). Unit boundaries C/D and D/E (see section 3.3) have been affected by intense mylonitization and seem to represent thrust planes. It is assumed that this tectonic event was contemporaneous with the fibrolitic layers (i.e. the second fabric generation) within the Mount Weston Gneiss.

As MARSH (1983a) already pointed out, the sediments may have been deposited on a pre-existing basement of Mount Weston Gneiss, i.e. they possibly represent an autochthonous unit. Indeed, high magnetite contents in Sub-Areas A -C suggest derivation of the sediments from eroded basement rocks similar to the Mount Weston Gneiss. This impression is supported by relict internal fabrics (s_i) within some minerals of the metasediments (Sub-Areas B -D). They are thought to derive from eroded metamorphics with an older tectonometamorphic history. Similarily, the single lens showing an old planar fabric (Fig. 30) most probably represents a detrital rock pebble.

Accepting an autochthonous nature for the lower Mount Gass Formation *sensu* MARSH (1983a), the contact between Sub-Areas C and D must represent a structural boundary of major importance (Fig. 42). Further W, in the north face of height „888" (Area 3), rotational fabrics indicate tectonic modification of the boundary between basement and sedimentary cover, while the more or less incompetent marble horizon about 500 m above the unconformity is not as heavily sheared as its equivalent in Area 2. Therefore, a ramp-like structure has to be considered in which the main shear plane rises from the basement/sediment boundary in Area 3 to an intra-sedimentary position (boundary C/D) in Area 2 (Fig. 42).

In Area 2, between Mount Weston and Pratts Peak, minor SE-vergent thrusting under retrograde conditions is documented in all sedimentary units. Since both NW-vergent and SE-vergent deformation are compressional, a major time break between these phases seems unlikely (which is supported by the distribution of radiometric ages, see Fig. 41). Thrusting took place preferentially in NW-dipping limbs of large-scale synclines where carbonate horizons parallel to the XY-plane of deformation allowed easy mylonitization. At present it is unclear whether northward tilting of the upper (northern) boundary of the Mount Weston Gneiss is a result of compressional folding or whether it was caused by late doming of the basement.

Due to insufficient abundance of suitable radioactive isotopes within the Stratton Gneiss, attempts to determine the radiometric age of this unit have not been successful (GREW & HALPERN 1979, PANKHURST et al.1983), which leaves some room for speculation. In the opinion of MARSH (1983a) the Stratton Gneiss represents a local basement on which sediments of the Nostoc Lake Formation were deposited. As shown in this study, however, the Stratton Gneiss appears to be the uppermost tectonostratigraphic unit in the northern Haskard Highlands (Fig. 42). Furthermore, the presence of agmatite at the contact with the

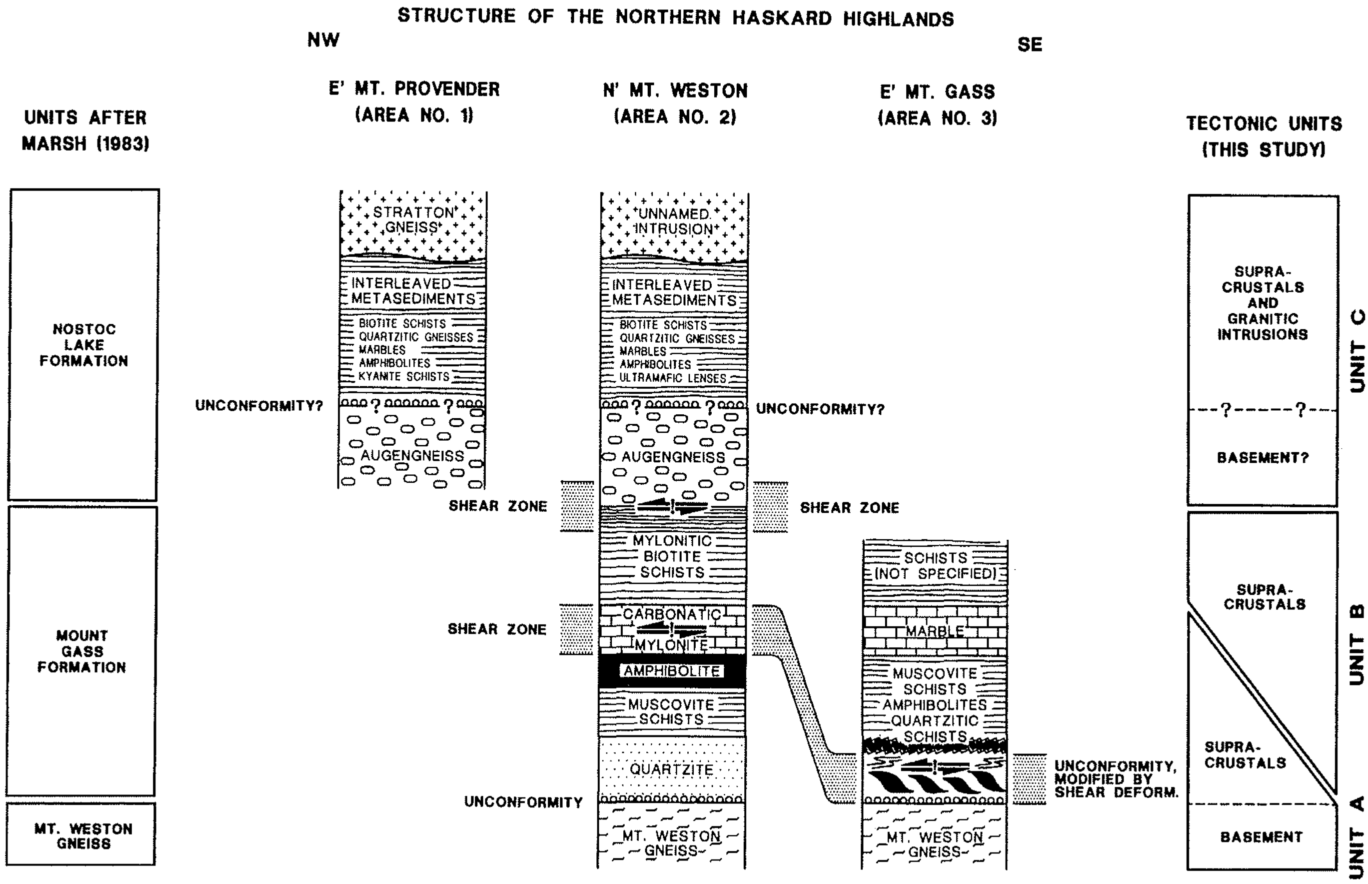

Fig. 42: Lithological and structural relationships between Areas 1-3 (see Fig. 25), northern Haskard Highlands (three centre columns). Left column refers to lithostratigraphic units of MARSH (1983a), right side shows tectonostratigraphic units (nappes?) as proposed in this study (informally labelled A to C).

Abb. 42: Mittlere drei Säulen: lithologische und strukturelle Beziehungen zwischen den Teilgebieten 1 bis 3 (vergl. Abb. 25), nördliche Haskard Highlands. Links außen: lithostratigraphische Einheiten nach MARSH (1983a). Rechts außen: mögliche tektonostratigraphische Einheiten (Teildecken?) als Resultat der vorliegenden Arbeit (informell als Einheit „A" bis „C" bezeichnet).

surrounding rocks suggests that the Stratton Gneiss is intrusive. A syn-metamorphic to late-metamorphic, i.e. Cambro-Ordovician age, is suggested by the present author.

Due to the lack of clear igneous contacts, the significance of the augen gneisses in the lower Nostoc Lake Formation is hard to assess. Their lower (southern) boundary crops out only in Area 2, where it represents a major shear plane. From the structural situation it is theoretically possible that the augen gneisses were part of the basement prior to sedimentation. However, Rb/Sr ages of 583 Ma (GREW & HALPERN 1979) and U/Pb-ages of 556-431 Ma (GREW & MANTON 1980) can also indicate intrusion early in the Cambrian metamorphic event, followed by tectonic reworking (flattening, shear zones, etc.).

Interpreting the structure of the northwestern Shackleton Range on a regional scale, MARSH (1983b) postulates a large „Lagrange Nappe" thrust on sediments of lower metamorphic grade (e.g. the Williams Ridge Formation further S). The present study confirms the general importance of syn-metamorphic, NW-directed shear deformation. In detail, however, an interpretation as a single, uniform nappe is not fully correct. In fact, several structural units were tectonically stacked during the Cambrian event, thus forming a pile of nappes. Even the Mount Weston Gneiss, which has been characterized as basement for autochthonous sediments further N, may represent a nappe unit with a sole thrust plane at the southern boundary of the gneiss complex (MARSH 1984). Post-tectonic heating within the thickened crust may be the reason for late intrusive activity, as well as for more or less static mineral growth within some of the metasediments.

4. SUMMARY

Two major tectonometamorphic events can be demonstrated in both the southern (Read Mountains) and northern (Haskard Highlands) parts of the Shackleton Range. Amphibolite facies metamorphism in the basement rocks of the Read Mountains occurred roughly between 1800 and 1650 Ma, with late granitic and granodioritic intrusions at about 1450 Ma. In the northern Shackleton Range, our knowledge of the history of the basement is not as detailed as in the S. According to radiometric dating, peak metamorphism in this region took place at about 1550 Ma. The kind of connections between the basement of the Read Mountains and the northern Shackleton Range remains unclear. The situation is complicated by radiometric ages of unknown significance between 2300 and 2700 Ma obtained for rocks from the Lagrange Nunataks and from the southern Haskard Highlands (PANKHURST et al. 1983).

Consolidation and the first phase of uplift and erosion of the Read Group terminated prior to Eocambrian sedimentation of the Watts Needle Formation. The results of the present study suggest an analogue unconformity in the northern Haskard Highlands. Furthermore, there is a striking lithological similarity between the Watts Needle Formation, and the probably autochthonous sediments on top of the Mount Weston Gneiss (i.e. the lower part of the Mount Gass Formation *sensu* MARSH 1983a; cf. KLEINSCHMIDT 1989). Similar rock sequences (quartzites, schists and carbonates resting on possible basement gneisses) have been reported, for example, from Mount Skidmore, Mount „E", the Lagrange Nunataks, and from Williams Ridge south of Mount Weston (MARSH 1983a, 1984).

The northern Haskard Highlands - and according to MARSH (1984) also the Lagrange Nunataks - were subject to syn-metamorphic NW thrusting at about 530 Ma. Minor SE backthrusting and large-scale upright folding occurred during later stages of compressional tectonics. Whereas the northern Haskard Highlands underwent syn-tectonic amphibolite facies metamorphism, the slightly younger (about 490 Ma), S- to SE-directed Mount Wegener Nappe was thrust onto more or less cool sediments and basement rocks. Only the nappe unit was subjected to pre-tectonic to syn-tectonic metamorphism under greenschist facies conditions, followed by more or less rapid cooling after the thrusting event. Up to now, the root area of the several nappe units and the region where the Mount Wegener Formation was deposited have not been localized precisely.

5. REGIONAL OUTLOOK AND PLATE TECTONIC MODELS

The basement rocks of the southern Shackleton Range were metamorphosed not much later than the mid-Proterozoic and may be regarded as part of the consolidated Antarctic craton thereafter. Emplacement of the Mount Wegener Nappe affected the underlying basement only to a minor extent. In contrast, the basement of the northern Shackleton Range was subject to intense tectonometamorphic reactivation during the Cambro-Ordovician, i.e. the time of the Ross Orogeny in the Transantarctic Mountains and in Victoria Land. Taking this situation into consideration, the geotectonic position of the Shackleton Range is inferred to be at the margin of the East Antarctic Craton (e.g. KLEINSCHMIDT & BRAUN 1991: Fig. 9).

There are remarkable similarities between the styles of thrusting in the Shackleton Range and in northern Victoria Land. In both areas, thrust planes directed towards the Antarctic Craton, as well as in the opposite direction, are known. A model of orthogonal subduction under the orogenic belt has been established for northern Victoria Land (KLEINSCHMIDT & TESSENSOHN 1987, FLÖTTMANN & KLEINSCHMIDT 1991a, b, KLEINSCHMIDT et al. 1993). The time gap of 30-40 Ma between thrusting in the northern and southern Shackleton Range corresponds well with findings that the „Ross Orogeny" probably does not represent a single event, but includes at least two phases of tectonometamorphic activity, and may even be a polyphase event (e.g. ROWELL et al. 1992). Thrusting at about 530 Ma in the northern Shackleton Range was contemporaneous with the Nimrod Event in the central Transantarctic Mountains, as interpreted by GOODGE et al. (1993a, b). Major structures resulting from transpressional tectonics, as reported by the latter authors, have not been found in northern Victoria Land (see FLÖTTMANN & KLEINSCHMIDT 1991b) or in the Shackleton Range.

According to studies in Neuschwabenland (western Dronning Maud Land), basement rocks N of the Shackleton Range were subjected intense tectonometamorphism during the Kibaran event at about 1100 Ma (e.g. SPAETH & FIELITZ 1987, JACOBS 1991, ARNDT et al. 1991). Cataclastic, NNW-directed shear zones in the Heimefrontfjella indicate minor tectonic reactivation during the "Pan-African" at about 500 Ma, i.e. more or less contemporaneous with the Ross Orogeny in Victoria Land and the Transantarctic Mountains, and with tectonometamorphism in the Shackleton Range.

New aspects of the Precambrian history of the Shackleton Range and surrounding areas emerge from the so-called SWEAT hypothesis (MOORES 1991, DALZIEL 1991, 1992). This model postulates a connection between North America (Laurasia) and Antarctica (Gondwana) prior to the opening of the Pacific Ocean, which seems to be corroborated by the age pattern of basement consolidation: The boundary between rocks affected by the main phase of metamorphism at about 1600-1500 Ma (Shackleton Range) and those affected by the one at about 1100 Ma (Dronning Maud Land) seems to continue between the Yavapai-Mazatzal region and the Grenvillian belt in North America (MOORES 1991: Fig. 3). The following additional aspects specific to the Shackleton Range should be mentioned: (i) Porphyritic granites in the Shackleton Range, as well as anorogenic A-type intrusions in SW North America, are late- to post-tectonic with respect to main tectonometamorphism of the basement, and have identical ages of slightly more than 1400 Ma (for the latter see ANDERSON 1983). Analyses of the Antarctic granites published by CLARKSON (1982a) suggest distinct geochemical similarities, e.g. relative enrichment in K and Fe. (ii) Crustal subsidence and subsequent sedimentation of the Watts Needle Formation were contemporaneous with the Late Proterozoic opening of the Pacific Ocean between Laurasia and Gondwana, as implied by the SWEAT hypothesis. (iii) If metasedimentary sequences in the northern Haskard Highlands are not equivalent to the Eocambrian Watts Needle Formation further S, the typical association of carbonatic and amphibolitic layers in the northern Shackleton Range suggests a possible correlation with Early Cambrian platform carbonates and metavolcanics in the central Transantarctic Mountains (STUMP 1992, 1993).

Tectonic activity during the Early Palaeozoic has been demonstrated in all major outcrop areas between northern Victoria Land on one side of Antarctica and western Dronning Maud Land on the other. This led previous authors to infer a single, continuous orogenic belt (Ross Orogen) following the margin of the Antarctic Craton (e.g. GUNN 1963, CRADDOCK 1972, GRIKUROV & DIBNER 1979, KLEINSCHMIDT & BRAUN 1991). Since palaeomagnetic data exclude rotation of the Shackleton Range as a block in Phanerozoic times (HOTTEN et al. 1991), however, Cambrian crustal shortening in the Shackleton Range definitely occurred perpendicular to the subduction direction in the Ross sector of Antarctica.

Sedimentary structures within the Watts Needle Formation (BUGGISCH et al. 1990, 1994b) indicate a marine basin with a long axis perpendicular to the Late Proterozoic passive continental margin in the Transantarctic Mountains. A Late Proterozoic rift branch connected to the proto-Pacific, which penetrates the Antarctic continent W of the Shackleton Range, represents a possible alternative to the classical „Ross" model. Rifting (and generation of oceanic crust?) would have been abandoned during the Cambrian, and closure of the basin led to N-S-directed compressional tectonics in the Shackleton Range („failed rift"). This model eliminates the Shackleton Range from discussions about processes at the Pacific margin of Gondwana. It is also independent of controversies about the approximate distribution of continents during the Precambrian and Cambrian („conventional" reconstructions, e.g. CRADDOCK 1982, LAWVER & SCOTESE 1987, LAWVER et al. 1991, *versus* the SWEAT hypothesis).

A different model emerges from recent publications by DALLA SALDA et al. (1992a, b), who postulate a connection between North and South America at about 570 Ma (see also DALZIEL 1992: Fig. 3). According to their reconstruction, the „southern Iapetus Ocean" opened between these two continents during the Early and mid-Cambrian, reaching the Shackleton Range with its narrow southern branch (DALLA SALDA et al. 1992b: Fig. 2). In this model, metamorphism and NNW-directed ductile deformation in the northern Haskard Highlands at about 530 Ma may be explained by southward subduction of Iapetus crust below the Antarctic Craton. Possible schematic cross sections of this stage are shown in BUGGISCH et al. (1990, 1994b). Following DALLA SALDA et al. (1992a, b), the Cambro-Ordovician Famatinian and Taconic orogens are products of the collision between North and South America and indicate final closure of the ocean at roughly 460-480 Ma. Late-metamorphic shears in the Haskard Highlands, nappe transport in the Read Mountains, and large-scale folding throughout the Shackleton Range may have the same cause.

One should keep in mind, however, that the models discussed above are purely speculative at present. This is especially true for the Laurasia-Gondwana connection proposed by the SWEAT hypothesis. A comparison of Proterozoic tectonic structures and crustal dynamics of the Shackleton Range with the Yavapai-Mazatzal region of SW North America will provide further information about this part of earth history. The Taconic Orogen in the Appalachians of North America, and Cambrian sediments on both sides of the postulated southern Iapetus Ocean, are certainly of interest with regard to early Phanerozoic development and should be tested in detail for possible analogies with the Shackleton Range.

6. ACKNOWLEDGEMENTS

The author thanks the Alfred Wegener Institute for Polar and Marine Research (Bremerhaven) and the Bundesanstalt für Geowissenschaften und Rohstoffe (Hannover) for the opportunity to participate in the 1987/88 expedition to the Shackleton Range, and for logistic support in the field. Financial grants by the Deutsche Forschungsgemeinschaft and the Johann Wolfgang Goethe University at Frankfurt (Main) are gratefully acknowledged. Thanks to all „GEISHAs", who made time in the field very productive and pleasant, and to Georg Kleinschmidt, Thomas Flöttmann and the tectonics working group at Frankfurt University for lively discussions.

References

Anderson, J.L. (1983): Proterozoic anorogenic granite plutonism of North America.- Geol. Soc. Am. Mem. 161: 133-154, Boulder.

Arndt, N.T., Todt, W., Chauvel, C., Tapfer, M. & Weber, K. (1991): U-Pb zircon age and Nd isotopic composition of granitoids, charnockites and supracrustal rocks from Heimefrontfjella, Antarctica.- Geol. Rundsch. 80: 759-778, Stuttgart.

Braun, H.-M., Kleinschmidt, G. & Spaeth, G. (1988): Strukturgeologie der Shackleton Range.- In: D.K. FÜTTERER (ed.), The Expedition ANTARKTIS-VI of RV „Polarstern" in 1987/1988.- Rep. Polar Res., 58: 208-217, Bremerhaven.

Buggisch, W., Kleinschmidt, G., Kreuzer, H. & Krumm, S. (1990): Stratigraphy, metamorphism and nappe-tectonics in the Shackleton Range (Antarctica).- Geodät. geophys. Veröff. I/15: 64-86, Berlin.

Buggisch, W., Kleinschmidt, G., Kreuzer, H. & Krumm, S. (1994a): Metamorphic and structural evolution of the southern Shackleton Range during the Ross Orogeny.- Polarforschung 63: 33-56

Buggisch, W., Kleinschmidt, G., Höhndorf, A. & Pohl, J. (1994b): Stratigraphy and facies of the (meta-) sediments in the Shackleton Range, Antarctica.- Polarforschung 63: 9-32

Clarkson, P.D. (1982a): Geology of the Shackleton Range. I. The Shackleton Range Metamorphic Complex.- Brit. Antarct. Surv. Bull. 51: 257-283, Cambridge.

Clarkson, P.D. (1982b): Tectonic significance of the Shackleton Range. - In: C. CRADDOCK (ed.), Antarctic Geoscience, 835-839; Madison (Univ. Wisconsin Press).

Clakrson, P.D. (1983): Geology of the Shackleton Range. II. The Turnpike Bluff Group.- Brit. Antarct. Surv. Bull. 52: 109-112, Cambridge.

Compston, W., Williams, I.S., Kirschvink, J.L., Zhang, Z. & Ma, G. (1992): Zircon U-Pb ages for the Early Cambrian time-scale.- Geol. Soc. London J. 149: 171-184.

Condie, K.C. (1989): Plate Tectonics & Crustal Evolution.- 3rd Edition, 476 p., Oxford (Pergamon).

Coney, P.S. (1980): Cordilleran metamorphic core complexes: An overview.- In: M.D. CRITTENDEN, P.J. CONEY & G.H. DAVIS (eds.), Cordilleran metamorphic core complexes.- Geol. Soc. Am. Mem. 153: 7-31, Boulder.

Cooper, J.A., Jenkins, R.J.F., Compston, W. & Williams, I.S. (1992): Ion-probe zircon dating of a mid-Early Cambrian tuff in South Australia.- Geol. Soc. London J. 149: 185-192.

Craddock, C. (1972): Antarctic tectonics. - In: R.J. ADIE (ed.), Antarctic Geology and Geophysics, 449-455; Oslo (Universitetsforlaget).

Craddock, C. (1982): Antarctica and Gondwanaland. - In: C. CRADDOCK (ed.), Antarctic Geoscience, 3-13, Madison (Univ. Wisconsin Press).

Dalla Salda, L.H., Cingolani, C.A. & Varela, R. (1992a): Early Paleozoic orogenic belt of the Andes in southwestern South America: Result of Laurentia - Gondwana collision?- Geology 20: 617-620, Boulder.

Dalla Salda, L.H., Dalziel, I.W.D., Cingolani, C.A. & Varela, R. (1992b): Did the Taconic Appalachians continue into southern South America?- Geology 20: 1059- 1062, Boulder.

Dalziel, I.W.D. (1991): Pacific margins of Laurentia and East Antarctica-Australia as a conjugate rift pair: Evidence and implications for an Eocambrian supercontinent.- Geology 19: 598-601, Boulder.

Dalziel, I.W.D. (1992): On the organization of American plates in the Neoproterozoic and the breakout of Laurentia.- Geol. Today 2: 237-241, Boulder.

Flöttmann, T. & Kleinschmidt, G. (1991a): Opposite thrust systems in northern Victoria Land, Antarctica: Imprints of Gondwana's Paleozoic accretion.- Geology 19: 45-47, Boulder.

Flöttmann, T. & Kleinschmidt, G. (1991b): Kinematics of major structures in North Victoria and Oates Lands, Antarctica.- Soc. Geol. Ital. Mem. 46: 273-282.

Golovanov, N.P., Milstein, V.E., Michajlov, V.M. & Shuljatin, O.G. (1979): Stromatolity i mikrofitolity chrebta Shekltona (Zapadnaja Antarktida).- Dokl. Akad. Nauk. SSSR 249: 977-979.

Goodge, J.W., Hansen, V.L. & Peacock, S.M. (1993a): Multiple petrotectonic events in high-grade metamorphic rocks of the Nimrod Group, central Transantarctic Mountains, Antarctica.- In: Y. YOSHIDA, K. KAMINUMA & K. SHIRAISHI (eds.), Recent Progress in Antarctic Earth Science, 203-209, Tokyo (Terra Sci. Publ.).

Goodge, J.W., Walker, N.W. & Hansen, V.L. (1993 b): Neoproterozoic-Cambrian basement-involved orogenesis within the Antarctic margin of Gondwana.- Geology 21: 37-40, Boulder.

Grew, E.S. & Halpern, M. (1979): Rubidium-Strontium dates from the Shackleton Range Metamorphic Complex in the Mount Provender area, Shackleton Range, Antarctica.- J. Geol. 87: 325-332, Chicago.

Grew, E.S. & Manton, W.I. (1980): Uranium-lead ages of zircons from Mount Provender, Shackleton Range, Transantarctic Mountains.- Antarct. J. US Rev. 15: 45-46.

Grikurov, G.E. & Dibner, A.F. (1979): Wosrast i strukturnoje polozenije osadotsnych tolsts w sapadnoj tsasti chrebta Shackleton (Antarktida).- Antarkt. Dokl. Kom. 18: 20-31.

Gunn, B.M. (1963): Geological structure and stratigraphic correlation in Antarctica.- N.Z.J. Geol. Geophys. 6: 423-443.

Hanmer, S. (1986): Asymmetrical pull-aparts and foliation fish as kinematic indicators.- J. Struct. Geol. 8: 111-122.

Hofmann, J., Kaiser, G., Klemm, W. & Paech, H.-J. (1980): K/Ar-Alter von Doleriten und Metamorphiten der Shackleton Range und der Whichaway Nunataks, Ost- und Südostumrandung des Filchner-Eisschelfs (Antarktis).- Z. geol. Wiss. 8: 1227-1232, Berlin.

Hofmann, J. & Paech, H.-J. (1983): Tectonics and relationships between structural stages in the Precambrian of the Shackleton Range, western margin of the East Antarctic craton.- In: R.L. OLIVER, P.R. JAMES & J.B. JAGO (eds.), Antarctic Earth Sciences, 183-189, Canberra (Austral. Acad. Sci.).

Hotten, R., Peters, M. & Spaeth, G. (1991): Paläomagnetismus proterozoischer und phanerozoischer Dolerite der Shackleton Range, Antarktika.- 16th Intern. Polar Meeting, Göttingen, Abstracts: 54 (German Soc. Polar Res.).

International Map of the World, Scale 1:100.000: Sheet U-26-13,14,15,16 (Flat Top); USSR, 1982.

Jacobs, J. (1991): Strukturelle Entwicklung und Abkühlungsgeschichte der Heimefrontfjella (Westliches Dronning Maud Land / Antarktika).- Rep. Polar Res., 97: pp. 141, Bremerhaven.

Kleinschmidt, G. (1989): Die Shackleton Range im Innern der Antarktis.- Geowiss. 7: 10-14, Weinheim.

Kleinschmidt, G. & Braun, H.-M. (1991): Gondwana's Pacific margin during the early Paleozoic: The Ross Orogen and its structure in the Shackleton Range and North Victoria Land (Antarctica).- In: H. ULBRICH & A.C. ROCHA CAMPOS (eds.), Gondwana Seven Proceedings, 19-32, Sao Paulo.

Kleinschmidt, G., Buggisch, W. & Flöttmann, T. (1993): Compressional causes for the early Paleozoic Ross orogen - Evidence from Victoria Land and the Shackleton Range.- In: Y. YOSHIDA, K. KAMINUMA & K. SHIRAISHI (eds.), Recent progress in Antarctic Earth science, 227-233, Tokyo (Terra Sci. Publ.).

Kleinschmidt, G. & Tessensohn, F. (1987): Early Paleozoic westward directed subduction at the Pacific margin of Antarctica.- In: G.D. MC KENZIE (ed.), Gondwana Six: Structure, tectonics, and geophysics, Am. Geophys. Union Monogr. 40: 89-105.

Lambert, R. St.J. (1983): Metamorphism and thermal gradients in the Proterozoic continental crust.- Geol. Soc. Am. Mem. 161: 155-166, Boulder.

Lawver, L.A. & Scotese, C.R. (1987): A revised reconstruction of Gondwanaland.- In: G.D. MC KENZIE (ed.): Gondwana Six: Structure, tectonics, and geophysics. - Am. Geophys. Union Monogr, 40: 17-23.

Lawver, L.A., Royer, J.-Y., Sandwell, D.T. & Scotese, C.R. (1991): Evolution of the Antarctic continental margin.- In: M.R.A. THOMSON, J.A. CRAME & J.W. THOMSON, (eds.), Geological evolution of Antarctica, 533-539, Cambridge (Cambridge Univ. Press).

Marsh, P.D. (1983a): The stratigraphy and structure of the metamorphic rocks of the Haskard Highlands and Otter Highlands of the Shackleton Range.- Brit. Antarct. Surv. Bull. 60: 23-43, Cambridge.

Marsh, P.D. (1983b): The late Precambrian and early Proterozoic history of the Shackleton Range, Coats Land.- In: R.L. OLIVER, P.R. JAMES & J.B. JAGO (eds.), Antarctic Earth Sciences, 190-193, Canberra (Austral. Acad. Sci.).

Marsh, P.D. (1984): The stratigraphy and structure of the Lagrange Nunataks, northern Fuchs Dome and Herbert Mountains of the Shackleton Range.- Brit. Antarct. Surv. Bull. 63: 19-40, Cambridge.

Miotke, F.-D. (1988): Microclimate, weathering processes and salt within ice-free continental Antarctica.- Polarforschung 58: 201-209, Bremerhaven.

Moores, E.M. (1991): Southwest U.S. - East Antarctic (SWEAT) connection: A hypothesis.- Geology 19: 425-428, Boulder.

Olesch, M. (1991): Metamorphism of basement rocks from the southern Shackleton Range.- 6th Intern. Symp. Antarct. Earth Sci. Abstracts: 456, Tokyo.

Paech, H.-J. (1985): Tectonic structures of the crystalline basement in the Shackleton Range, Antarctica. - Z. geol. Wiss. 13: 309-319, Berlin.

Paech, H.-J., Hahne, K. & Maass, I. (1991): Sedimentological and tectonical results on sedimentary rocks outcropping at the southern flank of the Shackleton Range, Antarctica.- Z. geol. Wiss. 19: 159-167, Berlin.

Paech, H.-J., Hahne, K. & Vogler, P. (1987): The palaeoenvironment of the Riphean Turnpike Bluff Goup sedimentation, Shackleton Range.- 5th Intern. Symp. Antarct. Earth Sci. Abstracts: 106, Cambridge.

Pankhurst, R.J., Marsh, P.D. & Clarkson, P.D. (1983): A geochronological investigation of the Shackleton Range.- In: R.L. OLIVER, P.R. JAMES & J.B. JAGO (eds.), Antarctic Earth Sciences, 176-182, Canberra (Austral. Acad. Sci.).

Passchier, C.W. & Simpson, C. (1986): Porphyroclast systems as kinematic indicators.- J. Struct. Geol. 8: 831-843, Oxford.

Platt, J.P. (1984): Secondary cleavages in ductile shear zones.- J. Struct. Geol. 6: 439-442, Oxford.

Ramberg, H. (1955): Natural and experimental boudinage and pinch-and-swell structures.- J. Geol. 63: 512-526.

Rex, D. (1972): K-Ar age determinations on volcanic and associated rocks from the Antarctic Peninsula and Dronning Maud Land. - In: R.J. ADIE (ed.), Antarctic Geology and Geophysics, 133-136, Oslo (Universitetsforlaget).

Roland, N.W., Kleinschmidt, G. & Buggisch, W. (1988): Geological expedition to the Shackleton Range - GEISHA 1987/88 - Nappe structure and a meteorite find.- BGR Circular 7: 3-20, Hannover.

Rowell, A.J., Rees, M.N. & Evans, K.R. (1992): Evidence of major Middle Cambrian deformation in the Ross Orogen, Antarctica.- Geology 20: 31-34, Boulder.

Schulze, P. (1989): Petrographie und Petrogenese der Gesteine von Beche Blade (Read Mountains) und Unnamed Nunatak (SSW Meade Nunatak, Pioneers Escarpment), Shackleton Range, Antarktis.- Unpubl. Diploma Thesis Univ. Würzburg, pp. 123.

Simpson, C. & Schmid, S.M. (1983): An evaluation of criteria to deduce the sense of movement in sheared rocks.- Geol. Soc. Am. Bull. 94: 1281-1288.

Spaeth, G. & Fielitz, W. (1987): Structural investigations in the Precambrian of Western Neuschwabenland, Antarctica.- Polarforschung 57: 71-92, Bremerhaven.

Stephenson, P.J. (1966): Geology. 1. Theron Mountains, Shackleton Range and Whichaway Nunataks (with a section on palaeomagnetism of the dolerite intrusions by D.J. Blundell).- Sci. Rep. Transantarct. Exped. 8: pp. 79, London.

Stump, E. (1992): The Ross Orogen of the Transantarctic Mountains in light of the Laurentia-Gondwana split.- Geol. Today 2: 25-31, Boulder.

Stump, E. (1993): Pre-Beacon tectonic development of the Transantarctic Mountains.- In: Y. YOSHIDA, K. KAMINUMA & K. SHIRAISHI (eds.), Recent progress in Antarctic Earth science, 235-240, Tokyo (Terra Sci. Publ.).

Weber, B. (1991): Microfossils in Proterozoic sediments from the southern Shackleton Range, Antarctica: a preliminary report.- Z. geol. Wiss. 19: 1851 -97, Berlin.

Wernicke, B. & Burchfiel, B.C. (1982): Modes of extensional tectonics.- J. Struct. Geol. 4: 105-115, Oxford.